

## 1 The formation of the Indo-Pacific montane avifauna

3 Andrew Hart Reeve<sup>a,\*</sup>, Jonathan David Kennedy<sup>a</sup>, José Martín Pujolar<sup>a,b</sup>, Bent Petersen<sup>c</sup>, Mozes P.  
4 K. Blom<sup>d</sup>, Per Alström<sup>e</sup>, Tri Haryoko<sup>f</sup>, Per G. P. Ericson<sup>g</sup>, Martin Irestedt<sup>g</sup>, Johan A. A. Nylander<sup>g</sup>,  
5 Knud Andreas Jönsson<sup>a</sup>

*<sup>8</sup> "Natural History Museum of Denmark, University of Copenhagen, DK-2100 Copenhagen Ø,  
<sup>9</sup> Denmark*

<sup>11</sup> <sup>b</sup>Centre for Ocean Life, DTU Aqua, Kemitorvet, Building 202, DK-2800 Kgs. Lyngby, Denmark

<sup>13</sup> *Section for Evolutionary Genomics, The GLOBE Institute, University of Copenhagen, DK-1353  
14 Copenhagen, Denmark*

<sup>16</sup> *<sup>d</sup>Museum für Naturkunde Berlin, Leibniz Institut für Evolutions- und Biodiversitätsforschung,*  
<sup>17</sup> *10115 Berlin, Germany*

<sup>19</sup> *Animal Ecology, Department of Ecology and Genetics, Evolutionary Biology Centre, Uppsala*  
<sup>20</sup> *University, Uppsala, Sweden*

*fMuseum Zoologicum Bogoriense Research Centre for Biology, National Research and Innovation Agency (BRIN), Jl. Raya Jakarta-Bogor Km 46, Cibinong 16911, Indonesia*

<sup>g</sup> Department of Bioinformatics and Genetics, Swedish Museum of Natural History, P.O. Box 50007, SE-104 05 Stockholm, Sweden

\*To whom correspondence should be addressed:  
a.reeve@snm.ku.dk

33 **ABSTRACT**

34 Mountain biotas have considerable conservation and research importance, but the formation of  
35 montane communities remains incompletely understood. Study of Indo-Pacific island faunas has  
36 inspired two main hypotheses for the generation of montane diversity. The first posits that montane  
37 populations arise via direct colonization from other mountain areas, while the second invokes  
38 recruitment from adjacent lowland populations. We sought to reconcile these apparently conflicting  
39 hypotheses by asking whether a species' ancestral geographic origin determines its mode of  
40 mountain colonization. To this end, island-dwelling passerine birds at the faunal crossroads between  
41 Eurasia and Australo-Papua provide an ideal study system. We recovered the phylogenetic  
42 relationships of the region's montane species, and used this information to reconstruct their  
43 ancestral geographic ranges, elevational ranges, and migratory behavior. We also performed  
44 genomic population studies of three super-dispersive montane species/clades with broad island  
45 distributions. Eurasian-origin species populated archipelagos via direct colonization between  
46 mountains. This mode of colonization appears related to ancestral adaptations to cold and seasonal  
47 Palearctic climates, specifically short-distance migration. Australo-Papuan-origin mountain  
48 populations, by contrast, evolved from lowland ancestors, and highland distribution mostly  
49 precludes their further colonization of island mountains. The patterns and processes revealed for  
50 this group are compatible with taxon cycles, a hypothesized process of lowland lineage expansion  
51 followed by montane relictualization. Collectively, our analyses explain much of the distributional  
52 variation within a complex biological system, and provide a synthesis of two seemingly discordant  
53 hypotheses for montane community formation.

54

55

56 **1. INTRODUCTION**

57 Mountains harbor a disproportionately great amount of earth's terrestrial biodiversity (Myers et al.,  
58 2000). Much of this montane diversity is concentrated in the tropics, where mountains' steep  
59 climatic gradients promote high elevational community turnover and endemism (Fjeldså et al.,  
60 2012). In the face of vast anthropogenic clearance of tropical lowland forests, tropical mountains  
61 represent last bastions of intact habitat in many parts of the world (Jepson et al., 2001), but these  
62 biotas now face climate change-driven extinction (La Sorte et al., 2010; Freeman et al., 2018).  
63 Despite their enormous conservation importance and a long history of intense scientific study (von

64 Humboldt & Bonpland, 1805), we lack answers to basic questions about how montane communities  
65 actually form. How does a species arrive on a mountaintop, and what is its fate once it does?

66 Our understanding of montane biodiversity formation owes much to study within  
67 island systems (Wilson, 1959, 1961; Ricklefs & Cox, 1978; Ricklefs & Bermingham, 2002; Mayr  
68 & Diamond 1976, 2001), and particularly the montane archipelagos of the Indo-Pacific. A striking  
69 and long recognized regional pattern is that individual montane species are often broadly distributed  
70 across many different islands and mountain ranges. The prevalence of these montane  
71 supercolonizers inspired the idea that direct colonization between mountain ranges is the key driver  
72 of montane community buildup (Stresemann, 1939; Mayr, 1944; Diamond, 1972; Mayr &  
73 Diamond, 1976). The opposite conclusion was reached by E. O. Wilson (1959, 1961), who argued  
74 that montane species form via ‘taxon cycles’ whereby dispersive lowland radiations gradually  
75 contract into the highlands to form endemic species restricted to single islands. These ideas are hard  
76 to reconcile, and molecular studies have found evidence of both processes (Jónsson et al., 2014,  
77 2017; Pepke et al., 2019; Cadena & Céspedes, 2020, Kennedy et al., 2022), even within a single  
78 mountain community (Merckx et al., 2015).

79 We investigated whether the variation in observed patterns can be explained by the  
80 ancestral source region of montane populations. Passerine birds have entered the many islands  
81 scattered between Eurasia and Australo-Papua from one or the other continental source. The  
82 establishment of montane island populations may follow fundamentally different processes  
83 depending on the long-term regional evolution of the parent lineage. Lineages from temperate  
84 regions may be more successful than tropical lineages at achieving broad and rapid colonization  
85 across mountain ranges (Lobo & Halffter, 2000; Donoghue, 2008; Merckx et al., 2015). We  
86 hypothesized that Eurasian-origin species, with preadaptations to cold and seasonal climates (e.g.,  
87 migration), colonize directly between island mountains, but that Australo-Papuan-origin species do  
88 not, and instead colonize mountains via recruitment from local lowland populations.

89 To test these hypotheses, we performed phylogenetic analyses to resolve the  
90 evolutionary relationships of the montane passerine avifauna of Wallacea and the Bismarck and  
91 Solomon Archipelagos (Fig. 1). We reconstructed the ancestral geographic range, elevational range,  
92 and migratory behavior of each species, and analyzed these together with newly compiled  
93 distributional datasets. To assess the processes inferred from species-level analyses, we  
94 implemented a novel bioinformatics method and conducted detailed phylogenomic population

95 studies of montane supercolonizers representing three of the broadest avian montane radiations in  
96 the region.

97

98

99 **2. RESULTS**

100 We identified 237 montane island populations (MIPs) distributed across 31 islands in Wallacea and  
101 the Bismarck and Solomon Archipelagos, representing 110 species, 47 genera, and 22 families  
102 (Tables 1 and S1; Supplementary File 2). Of the 110 species with MIPs, 80 were placed  
103 phylogenetically (Tables 1 and S1). The 80 species were analyzed within the context of 23 different  
104 clades, for which we used five tree files from published studies, one publicly available alignment  
105 file, and 17 trees generated specifically for this study (Supplementary File 3). The 23 clades contain  
106 787 ingroup tips representing 695 species. Ingroup species per clade range from 4 to 185 (mean =  
107 30), and mean species sampling completeness per clade is 90%. The trees produced for this study  
108 were highly congruent with the latest published molecular analyses for the relevant groups. Tree  
109 files are available from [pending]. We used these trees to perform ancestral state reconstructions of  
110 geographic range, elevational range, and migratory behavior (Table S2; Supplementary File 4).

111 We defined the geographic origin of the 80 focal species as follows: 31 Eurasian-  
112 origin species representing 100 MIPs from 11 genera and 7 families; 25 Australo-Papuan-origin  
113 species representing 33 MIPs from 14 genera and 5 families; and 24 species not clearly tracing back  
114 to either focal source area, representing 41 MIPs from 14 genera and 11 families (Tables 1 and S1;  
115 Supplementary File 2). Locating tree nodes representing continental ancestors (“Ancestral Source  
116 Nodes” – see Section 4.4) involved counting back 1–10 nodes (mean = 4.2) from tips. Thirty-four  
117 unique Ancestral Source Nodes were identified from among the 56 Eurasian-origin and Australo-  
118 Papuan-origin species (some species traced back to the same continental ancestor). Mean age of  
119 Ancestral Source Nodes for all species was 7.7 Ma.

120 Eurasian-origin species generally trace back to ancestors with distributions spanning  
121 both Indomalaya and the Palearctic (Supplementary File 5). Indomalaya is the geographically  
122 proximate species source pool feeding the archipelagos. The Indomalayan signature varies, but is  
123 >50% for most nodes older than 5 Ma. The root nodes of all clades have a 75–100% probability of  
124 Indomalayan occurrence, except for *Ficedula* (Muscicapidae; c. 40%). The Palearctic signature  
125 either rises markedly (though variably) back through time, or is consistently high (>75%). The root

126 nodes of all clades have a 75–100% probability of Palearctic occurrence, except for *Brachypteryx*  
127 (Muscicapidae; c. 60%).

128

129 **2.1. Statistical analyses**

130

131 **2.1.1. Montane vs. lowland ancestry**

132 Eurasian-origin species with MIPs evolved from predominantly montane continental ancestors  
133 (mean probability of montane ancestry 0.93), whereas Australo-Papuan-origin species evolved from  
134 predominantly lowland ancestors (mean probability of montane ancestry 0.23) (Fig. 2). Median  
135 probabilities of montane ancestry for the two groups differed significantly (Mann-Whitney U-test:  
136  $W = 738, p < .001$ ).

137

138 **2.1.2. Establishing multiple MIPs**

139 Eurasian-origin species have a higher number of MIPs than Australo-Papuan-origin species (Mann-  
140 Whitney U-test:  $W = 581.5, p < .001$ ) (Fig. 3; Tables S3 and S4). This is also the case in separate  
141 regional analyses of Wallacea and the Bismarcks/Solomons ( $p < .05$  in both cases). A higher  
142 proportion of Eurasian-origin species have multiple MIPs (0.65) than do Australo-Papuan-origin  
143 species (0.20):  $X^2 (1, N=56) = 9.4, p < .01$ . For individual regions, this relationship is statistically  
144 significant in the Bismarcks/Solomons ( $p < .05$ ), but not in Wallacea ( $p > .05$ ). Eurasian-origin  
145 species with continental populations ( $n = 13$ ) have higher numbers of MIPs than species restricted  
146 solely to islands ( $n = 18$ ) (Mann-Whitney U-test:  $W = 182.5, p < 0.01$ ; Fig. S1).

147

148 **2.1.3. MIPs and lowland island populations (LIPs)**

149 The proportion of MIPs to total island populations (MIPs + LIPs) is higher for Eurasian-origin  
150 species (mean = 0.90) than for Australo-Papuan-origin species (mean = 0.44); median values  
151 differed significantly (Mann-Whitney U-test:  $W = 194, p < 0.001$ ) (Fig. S2).

152 Eurasian-origin and Australo-Papuan-origin species show very different patterns in  
153 numbers of MIPs vs. total island populations (Fig. 4). Eurasian-origin species maintain consistently  
154 montane distributions as they radiate across archipelagos. This pattern does not fit with  
155 conventional taxon cycle theory. There are few examples of species with low proportions of MIPs  
156 to total island populations which might represent early- or mid-stage taxon cycles. The species with  
157 high proportions of MIPs to total island populations cannot be considered to represent late-stage

158 taxon cycles because they have high numbers of MIPs. In contrast, Australo-Papuan-origin species  
159 show an overall pattern that is entirely compatible with taxon cycles. The hypothesized signatures  
160 of early stages (many lowland populations), middle stages (a mix of lowland and montane  
161 populations), and late stages (one or few montane populations with no lowland populations) are all  
162 represented. Australo-Papuan-origin species that are entirely montane within the focal archipelagos  
163 are older than those having both MIPs and LIPs, in accordance with predictions of the taxon cycle.  
164 We tested this by defining species age as the estimated time to divergence from a sister species or  
165 clade in our phylogenetic trees. The average node age of species where the proportion of MIPs to  
166 total island populations = 1 (n=16; mean = 5.80 Ma; median = 5.46 Ma) is higher than average node  
167 age of species where that proportion < 1 (n=9; mean = 2.36 Ma; median = 1.30 Ma); this difference  
168 is significant (Mann-Whitney U-test:  $W = 22, p < 0.01$ ).  
169

#### 170 **2.1.4. Migration**

171 Slightly over half of the ancestors of the 31 Eurasian-origin species had short-distance migrant  
172 populations, and very few had long-distance migrant populations (Fig. S3, Table 2). Most had at  
173 least some sedentary populations across their ranges. The ancestors of the 25 Australo-Papuan-  
174 origin species were overwhelmingly sedentary, with very few short-distance migrant populations  
175 and no long-distance migrant populations (Table 2). Comparison of median ancestry probabilities  
176 confirmed that Eurasian-origin ancestors had a higher probability of making migratory movements  
177 (Mann-Whitney U-test:  $W = 744, p < .001$ ).

178 Species with short-distance migrant populations have higher numbers of MIPs than  
179 species that are sedentary throughout their range (Fig. 5). Short-distance migrant populations occur  
180 only outside the focal archipelagos, and no species with MIPs have long-distance migrant  
181 populations. When considering all species with MIPs, species with short-distance migration (n = 12)  
182 have a mean of 6.17 MIPs, and entirely sedentary species (n = 98) have a mean of 1.67 MIPs.  
183 Median values for the two groups differed significantly (Mann-Whitney U-test:  $W = 142.5, p <$   
184  $.001$ ). Among Eurasian-origin species, species with short-distance migration (n=8) have a mean of  
185 5.38 MIPs, and entirely sedentary species (n=23) have a mean of 1.67 MIPs. Again, median values  
186 for the two groups were significantly different (Mann-Whitney U-test:  $W = 147, p < .05$ ).  
187

#### 188 **2.1.5. Competitive pressure in the lowlands**

189 A higher proportion of Australo-Papuan-origin MIPs face potential competition from lowland  
190 congeners (0.36) than do Eurasian-origin MIPs (0.06) ( $X^2$  (1, N=133) = 14.3,  $p < .001$ ). Similarly, a  
191 higher proportion of Australo-Papuan-origin MIPs face potential competition from lowland species  
192 from the same family (0.73) than do Eurasian-origin MIPs (0.36) ( $X^2$  (1, N=133) = 12.1,  $p < .001$ ).  
193 Nevertheless, competition from lowland relatives does not appear to be the sole factor driving MIP  
194 formation for Australo-Papuan-origin species, because a number of Australo-Papuan MIPs lack  
195 close relatives in the lowlands.

196

### 197 **2.1.6. Phylogenetic null models**

198 We used phylogenetic null models to assess how well the empirical patterns of the tests described in  
199 Sections 4.5.1–4.5.5 could be replicated based on data simulated under a Brownian motion model of  
200 evolution (Table S5). For five of eight analyses, our empirical F statistics are significantly greater  
201 than those derived from the simulated null datasets. However, the pattern that Eurasian-origin  
202 species have more MIPs than Australo-Papuan species can be reproduced upon simulating the data  
203 using Brownian motion alone. This is true with regard to all islands ( $p = .07$ ), for Wallacea alone ( $p$   
204 = .16), and for Bismarcks/Solomons alone ( $p = .08$ ). One potential source of this strong  
205 phylogenetic signal is the tight phylogenetic clustering of certain species with MIPs, most  
206 obviously the Indo-Pacific *Phylloscopus* leaf warbler clade that has spawned 11 MIPs in just four  
207 million years (see Section 2.2). However, this does not seem to be the source of the signal, because  
208 the average number of MIPs within these species clusters (e.g., a mean of 2.1 MIPs per species  
209 across all islands in the Indo-Pacific *Phylloscopus* leaf warbler clade) is similar to the average  
210 across all species within their respective geographic groups (mean = 3.2 MIPs per species across all  
211 islands). Rather, the source of the phylogenetic signal appears to derive from the deep structure of  
212 the relationships of all species in the analysis: it is clear that our comparison of Eurasian and  
213 Australo-Papuan avifaunas is nearly equivalent to a comparison of the major passerine clades  
214 Passerides (Eurasia) and Corvides/Meliphagides (Australo-Papua). A strong phylogenetic signal is  
215 therefore inherent to our study.

216

### 217 **2.2. Population studies of montane supercolonizers**

218 Twelve trees representing four phylogenetic analyses for each of the three montane supercolonizers  
219 (Fig. 6) are presented in Figs. S4–S15. Discussion of the results centers around the dated  
220 supermatrix analyses, which have near-complete taxon coverage, and the genomic maximum

221 likelihood (ML) trees based on concatenated data, which are highly resolved. The genomic species  
222 trees are entirely congruent with the genomic ML trees, but support values are slightly lower.  
223 Mitogenome trees are variously well resolved, and in some cases recover highly supported  
224 relationships conflicting with the other genomic analyses, which may reflect introgression between  
225 populations (Rheindt et al., 2020).

226 For all groups, to varying degrees, we found that current taxonomic treatments do not  
227 accurately reflect phylogenetic relationships. Overall, the population studies reinforce the results  
228 obtained using the species-level ancestral state reconstructions (Section 2.1) in showing that the  
229 three montane supercolonizers evolved from continental Asian ancestors that were montane with a  
230 tendency for short-distance migration. The analyses strongly support the idea that all three  
231 radiations proceeded eastwards out of continental Indomalaya following a stepping stone pattern of  
232 sequential island colonization. All radiations included separate expansions 1) across the Lesser  
233 Sundas, and 2) via Sulawesi into the Moluccas (and in the case of the Indo-Pacific *Phylloscopus*  
234 leaf warblers, further into Melanesia). Radiations varied in tempo and duration, but took place  
235 mostly or entirely within the Pleistocene. The small number of lowland populations of montane  
236 supercolonizers were found to represent a few individual shifts away from an otherwise montane  
237 distribution. Two populations of altitudinal migrants belong to early branching clades within their  
238 respective groups, further suggesting an ancestral propensity for short-distance migration among  
239 montane supercolonizers. Detailed results of the population studies are presented in Supplementary  
240 File 1.

241  
242  
243 **3. DISCUSSION**

244 Our study provides a synthesis that reconciles contrasting hypotheses about the formation of Indo-  
245 Pacific montane diversity. We find that montane island populations' (MIPs) modes of colonization,  
246 and their potential for further montane colonizations, are governed by the long-term regional  
247 evolution of their parent lineages. Eurasian-origin MIPs derive from montane continental ancestors,  
248 while Australo-Papuan-origin MIPs evolved from lowland continental ancestors. Montane  
249 distribution does not inhibit further montane colonization by Eurasian-origin species, but it does for  
250 Australo-Papuan-origin species. Here we seek to characterize and explain these dichotomous  
251 processes.

253 **3.1. Temperate vs. tropical origins**

254 Our study compares Eurasian and Australo-Papuan avifaunas, but it is also a comparison between  
255 avifaunas of temperate (Eurasian) versus tropical (Australo-Papuan) climates. This may not be  
256 immediately intuitive, because tropical Southeast Asia serves as a gateway for colonization of the  
257 focal islands. However, our ancestral geographic and elevational range reconstructions show that  
258 virtually none of the montane diversity in the focal islands derives from lowland Indomalaya (Fig.  
259 2; Supplementary File 4). The ancestors of Eurasian-origin MIPs occurred in cool montane climates  
260 (Fig. 2) with ranges spanning both the Palearctic and Indomalayan realms (Supplementary File 5).  
261 Lowland Indomalayan lineages, on the other hand, may actually generate montane populations  
262 within Indomalaya itself in a similar way to lowland Australo-Papuan lineages; studies from the  
263 Greater Sundas provide examples of range-restricted montane endemics arising via recruitment  
264 from regional lowland clades (Merckx et al., 2015), sometimes driven by displacement by lowland  
265 congeners (reviewed in Sheldon et al., 2015). However, lowland Indomalayan lineages differ  
266 strikingly from lowland Australo-Papuan lineages in their near complete failure to generate MIPs in  
267 the focal archipelagos.

268

269 **3.2. The different fates of montane island populations**

270 For Eurasian-origin species, mountains often represent stepping stones to additional montane  
271 colonizations, but for Australo-Papuan-origin species they represent dead-ends for further dispersal.  
272 Both Eurasia and Australo-Papua have substantial montane avifaunas distributed across broad  
273 elevational gradients. Australo-Papuan montane species can colonize the disjunct mountain ranges  
274 of New Guinea (Diamond, 1972; Pujolar et al., 2022), but they are extremely poor at crossing deep  
275 water barriers. The different colonization processes of Eurasian-origin versus Australo-Papuan-  
276 origin birds appears to be rooted in the temperate/tropical dichotomy in our study system, aligning  
277 with previous observations that lineages from regions with cold and seasonal climates are adept at  
278 colonizing disjunct mountain ranges (Lobo & Halffter, 2000; Donoghue, 2008; Merckx et al.,  
279 2015). Eurasian montane species, with high diversity in the Sino-Himalaya, face much more  
280 extreme annual climate variation than their Australo-Papuan counterparts concentrated near the  
281 equator in New Guinea. This contrast has existed for millions of years, and has promoted mobility  
282 in the form of elevational migration among Eurasian montane species (Table 2; Fig. S3). We show  
283 that a capacity for short-distance migration can help predict whether a species or clade experiences  
284 a mountaintop as a stepping stone or a dead end (Fig. 5).

285 It may be conserved morphological or cognitive adaptations for short-distance  
286 migration, or both, that aid establishment of multiple MIPs. Ancestral short-distance migration  
287 specifically — as opposed to long-distance migration — may be an important promoter of  
288 mountain-to-mountain colonization. Our reconstructions show virtually no trace of long-distance  
289 migration among the ancestral source nodes of species with MIPs (Fig. S1), and long-distance  
290 migration has been shown to actually constrain colonization of new regions (Böhning-Gaese et al.,  
291 1998). Nomadism driven by granivory, nectarivory, or frugivory may provide a similar catalyst.  
292 The few non-passerines that have colonized mountains on multiple islands in the focal archipelagos  
293 are parrots (*Charmosyna*, *Micropsitta*) and pigeons (*Gymnophaps*) that make nomadic wanderings  
294 in search of fruit or flowers (Collar, 1997; Baptista et al., 1997).

295 Our phylogenetic null models (Table S5) underscore that our comparison of Eurasia  
296 vs. Australo-Papuan birds is, to a high degree, a comparison between the large passerine clades  
297 Passerides (Eurasia), and Corvides and Meliphagides (Australo-Papua). All three clades initially  
298 evolved in Australia, but Passerides quickly expanded into Eurasia c. 30 Ma and then radiated  
299 across the globe (Oliveros et al., 2019). This raises the intriguing possibility that Eurasian species'  
300 high propensity for mountain colonization is related to ancestral traits of Passerides that evolved  
301 prior to, or even facilitated the clade's initial expansion into Eurasia. The global expansion of  
302 Passerides has been attributed to a possible early evolution of increased thermal flexibility and  
303 short-duration social pairing for breeding (reviewed in Christidis et al., 2020). However, as we  
304 demonstrate, the ability to colonize directly between mountains is disproportionately manifested  
305 among species that come from a specific temperate evolutionary background, and that have  
306 behavioral traits reflective of that ancestry (i.e., short-distance migration). This speaks strongly for  
307 regional evolution as the causative mechanism.

308

### 309 **3.3. Mechanisms driving montane distributions**

310 Why species acquire and retain montane distributions remains an open question (Jankowski et al.,  
311 2013), but our study system provides new insights. Competition from closely related species may  
312 drive upward range shifts in Australo-Papuan-origin MIPs, which often share islands with lowland  
313 species from the same genus and/or family. This is not the case for Eurasian-origin MIPs, which  
314 mostly do not have close relatives in the lowlands (Section 2.1.5). Clues about the mechanisms  
315 driving montane distributions for Eurasian-origin MIPs can be found by looking at their conspecific  
316 populations in continental Asia. Species with altitudinal migrant populations in the Sino-Himalayan

317 region are among the most successful mountain-to-mountain colonizers in the focal archipelagos.  
318 These Sino-Himalayan populations spend much of the year in the lowlands, indicating that montane  
319 distribution is not a physiological imperative, nor is it driven by susceptibility to lowland pathogens  
320 (Bodawatta, 2020). Rather, mid-elevation peaks in arthropod abundance may drive songbirds'  
321 montane distributions in that region (Price et al., 2014). Diamond (1975) argues that Island Thrush  
322 *Turdus poliocephalus*, a Eurasian-origin montane supercolonizer, has an elevational range that is  
323 governed by levels of diffuse competition on different islands; i.e., it is a weak competitor that is  
324 restricted to mountains where overall bird species diversity is high, but occurs into the lowlands on  
325 species-poor islands. This explanation cannot be applied generally to the entire assemblage of  
326 Eurasian-origin species with MIPs, nearly half of which have tropical and subtropical continental  
327 populations from species-rich mid-montane communities. Further, if diffuse competition drives  
328 montane distributions, it is unclear why montane species have not colonized the myriad small, low,  
329 species-poor islands in the focal region (Supplementary File 2). Avoidance of high nest predation  
330 pressure in the lowlands (e.g., from *Boiga* snakes) may be a more parsimonious explanation for  
331 these patterns, and is a mechanism that is increasingly thought to drive montane species  
332 distributions (Skutch, 1985; Boyle, 2008; Jankowski et al., 2013).

333

### 334 **3.4. Taxon cycles**

335 There is no single agreed-upon definition of taxon cycles (Wilson, 1961; Ricklefs & Birmingham,  
336 2002), and arguments for their existence necessarily hinge upon inference of range shifts, niche  
337 shifts, and extinctions which mostly leave no direct evidence. However, the patterns we recover  
338 among Australo-Papuan-origin species fit with its basic idea that broad lowland radiations colonize  
339 archipelagos, gradually move into the mountains of larger islands while experiencing extinctions on  
340 smaller islands, and leave behind relictual species restricted to the mountains of single islands. We  
341 recover the hypothesized lowland-to-highland distributional shift (Fig. 2), and find that this  
342 coincides with a diminished capacity for further colonization (Fig. 3). Australo-Papuan-origin  
343 species never have many montane populations in the focal archipelagos, but can have few or many  
344 lowland populations (Figs. 4, S2), and this may reflect taxon cycles in varying stages of  
345 advancement. Eurasian-origin MIPs clearly did not arise by this process; they retain an ancestral  
346 montane distribution as well as the ability to colonize additional island mountains (Figs. 4, S2).  
347 Eurasian-origin archipelagic radiations do appear to slow down over time, based on the observation  
348 that species with continental occurrence have more MIPs than species restricted to archipelagos

349 (Fig. S1). Whether this slowing predictably leads to lineage relictualization, either in mountains or  
350 in lowlands, is unclear.

351 The taxon cycle idea predicts consistent upward range shifts over time, and this has  
352 the potential to confound our elevational range reconstructions of ancestral source nodes. If a clade  
353 consists mostly of montane late-stage taxon cycle relicts, then its deeper nodes will be incorrectly  
354 reconstructed as montane. This issue mostly does not manifest itself in the reconstructions of  
355 Australo-Papuan groups (Supplementary File 4) because modern lowland distribution is so  
356 pervasive across the relevant clades. It is more pertinent for the reconstructions of Eurasian groups  
357 (Supplementary File 4), which indicate montane distributions for virtually all ancestral source nodes  
358 (Fig. 2). Nevertheless, it does not seem plausible that this issue has biased the results because that  
359 would require that nearly all MIPs and the species in their constituent clades represent late-stage  
360 taxon cycles, when in fact many clades are recently evolved and speciose, and contain species with  
361 broad montane distributions. Further, our population studies of montane supercolonizers (Figs. S4–  
362 S15) reveal formation of montane populations until very recent times, so taxon cycles would have  
363 to be extremely fast as well as highly synchronized. The parsimonious explanation for this pattern is  
364 that species retained the montane distribution of their Eurasian ancestors.

365

### 366 **3.5. Impact of Pleistocene cooling on montane archipelago colonization**

367 Montane island populations face a double barrier to dispersal, with both lowland areas and expanses  
368 of water presenting formidable obstacles (Stresemann, 1939). However, the overall colder climate  
369 and repeated glacial periods in the Pleistocene would have weakened these barriers through the  
370 downslope expansion of montane forest (Garg et al., 2020), and the formation of land bridges  
371 between some islands due to lower sea levels. Low intervening islands likely hosted cool forests  
372 suitable for montane species, further facilitating their dispersal through archipelagos (White &  
373 Bruce, 1986; Kershaw et al., 2011). While cooler climates cannot have completely eliminated  
374 lowland competition, predation, and pathogen pressure, the Pleistocene almost certainly brought  
375 improved opportunities for colonization between island mountains. Eurasian-origin and Australo-  
376 Papuan-origin species reacted very differently to these opportunities, however. Eurasian-origin  
377 montane species made numerous colonizations of archipelagos, and established many MIPs during  
378 this time. This can be inferred if we assume that most intra-species population divergences are  
379 younger than 2.6 Ma. Our population studies of montane supercolonizers (Figs. S4–S15) support  
380 this, indicating that the vast majority of colonizations across deep and shallow water barriers

381 occurred during the Pleistocene. Australo-Papuan-origin species, by contrast, had almost no  
382 perceptible reaction to Pleistocene cooling. Only two Australo-Papuan-origin species have  
383 continental populations, indicating that there was minimal colonization of archipelagos by montane  
384 species in this grouping during this time. There are few species with multiple MIPs, and among  
385 these, MIP numbers are low (Fig. 3; Tables S3, S4). Therefore, while Pleistocene cooling  
386 potentially facilitated inter-island colonization by these species' lowland ancestors, it does not seem  
387 to have promoted colonization by montane populations. In addition to the lower dispersal capacity  
388 that we infer for Australo-Papuan-origin MIPs, the potentially higher levels of competition they  
389 face from lowland relatives may have contributed to preserve the isolation of montane populations  
390 during the Pleistocene.

391

### 392 **3.6 Conclusion**

393 The complex patterns of earth's montane biodiversity have inspired conflicting hypotheses about  
394 how it evolved. We reconcile these hypotheses by demonstrating that avifaunas from different  
395 continents follow fundamentally different processes to generate montane populations. This  
396 dichotomy reflects an important divide between temperate and tropical lineages. As our knowledge  
397 of the phylogenetic relationships of species rapidly improves, it will be increasingly feasible to  
398 investigate how the regional evolution of lineages has shaped contemporary global biodiversity  
399 patterns.

400

401

## 402 **4. METHODS**

403 Taxonomic classification follows IOC v 9.2 (Gill & Donsker, 2019) for all analyses unless  
404 otherwise noted (see Supplementary File 6).

405

### 406 **4.1. Defining montane island populations**

407 In this study we focus on the passerine birds of Wallacea and the Bismarck and Solomon  
408 Archipelagos. Geographic boundaries of Wallacea follow those of Coates & Bishop (1997), and we  
409 follow Dutson's (2011) regional delimitation of the Bismarcks and Solomons.

410 We are interested in species with populations that are restricted entirely to the  
411 mountains. A centrally important unit in this study is the montane island population ("MIP"),  
412 defined as an individual island population that occurs in the mountains but not at sea level (i.e., has

413 not been recorded below 100 masl). This is the definition used by Mayr and Diamond (2001) to  
414 classify montane populations in Northern Melanesia. Our focus is on populations that cannot persist  
415 at sea level, and therefore this definition is not intended to distinguish populations that reach the  
416 highlands from those restricted to the lowlands (although it does broadly have that effect). For  
417 example, a population occurring at 0–2,000 masl is considered “lowland,” while a population  
418 occurring at 500–1,500 masl is considered “montane.”

419 We identified MIPs using distributional information from Coates & Bishop (1997) for  
420 Wallacea, and from Dutson (2011) for the Bismarcks and Solomons. This dataset was further  
421 refined after a careful review of subsequently published primary literature on the respective regions  
422 (Supplementary File 2). Certain small islands within the focal region probably host one or more  
423 MIPs, but were excluded because available distributional data were too limited to accurately  
424 identify them. Certain MIPs known from very few records presumably do reach the lowlands, given  
425 the species’ lowland distributions throughout the rest of their ranges; these were removed from  
426 consideration. MIPs of non-breeding migrants were not considered, and there are no very clear  
427 examples of such populations.

428

#### 429 **4.2. Phylogenetic trees for ancestral state reconstructions**

430 We placed species with MIPs in species-level phylogenetic trees to allow reconstruction of  
431 ancestral geographic range, elevational range, and migratory behavior. We obtained tree files from  
432 published analyses for some groups, but otherwise produced new trees using both sequence data  
433 from GenBank (Supplementary File 6) and data newly generated for this study (see Sections 4.6–  
434 4.8). Clade limits were defined with the goal of determining Eurasian or Australo-Papuan origin (or  
435 lack thereof) for species with MIPs. The clades as defined were approximately 5–15 Ma old. Each  
436 encompassed no more than one family. We did not run phylogenetic analyses for clades in which  
437 taxonomic coverage of sequence data was very incomplete, or for clades where the latest molecular  
438 studies fail to resolve species relationships to a useful degree.

439 Phylogenetic analyses were performed using 1–6 genes per clade (see Supplementary  
440 File 6). Both nuclear and mitochondrial genes were used for three clades of particular interest (see  
441 Section 4.6), and for an additional clade for which we obtained a publicly available alignment file.  
442 Analyses of the remaining clades were built upon a subset of 1–2 mitochondrial genes, which are  
443 phylogenetically highly informative at the recent timescales with which we are concerned.  
444 Individual gene alignments were built using MAFFT (Katoh et al., 2002), as implemented in

445 SEAVIEW (Gouy et al., 2010). We analyzed individual gene partitions in BEAST (v.1.8.4;  
446 Drummond et al., 2012) as a preliminary quality check of the sequence data. We analyzed the  
447 concatenated datasets, partitioned by genes in BEAST, using the GTR nucleotide substitution  
448 model for mitochondrial genes (unlinked), and the HKY nucleotide substitution model for nuclear  
449 genes (unlinked). We used a relaxed uncorrelated lognormal distribution for the molecular clock  
450 model (all genes unlinked), and assumed a Birth-death speciation process as a tree prior. For each  
451 clade, the Markov chain Monte Carlo (MCMC) algorithm was run three times for 100 million  
452 iterations, with trees sampled every 10,000th generation. Convergence of individual runs was  
453 assessed using Tracer (v.1.6; Rambaut et al., 2014), ensuring all ESS > 200, and graphically  
454 estimating an appropriate burn-in (10 million generations in most cases). In cases where individual  
455 runs failed to converge, nucleotide substitution and molecular clock models were replaced with  
456 simpler models. TreeAnnotator (v.1.8.2; Rambaut & Drummond, 2015) was used to summarize a  
457 single maximum clade credibility (MCC) tree using mean node heights. To obtain absolute dates,  
458 we followed Lerner et al. (2011) and applied a rate of 0.007 substitutions per site per lineage (1.4%)  
459 per Ma to cytochrome *b* (cyt-*b*) data; 0.008 substitutions per site per lineage (1.6%) per Ma to  
460 cytochrome *c* oxidase I (COI) data; 0.0145 substitutions per site per lineage (2.9%) per Ma to  
461 NADH dehydrogenase 2 (ND2) data; and 0.012 substitutions per site per lineage (2.4%) per Ma to  
462 NADH dehydrogenase 3 (ND3) data.

463 We compared our trees individually against the most current and comprehensive  
464 published trees available for the respective groups, and evaluated congruence between well-  
465 supported nodes (posterior probability > 0.98) in those trees with our own results. Details on  
466 individual analyses are in Supplementary File 6, including taxonomic coverage per clade, gene sets,  
467 departures from default analysis settings, and publications referenced for tree topologies.  
468

#### 469 **4.3. Ancestral state reconstructions**

470 We used the R package BioGeoBEARS (Matzke 2013a, 2013b) to reconstruct geographic range,  
471 elevational range, and migratory behavior across the generated trees (Section 4.2). We compared  
472 Dispersal-Extinction Cladogenesis (DEC) models (Ree & Smith, 2008) with and without an  
473 additional free parameter (+j) that allows for founder-effect speciation. These models are typically  
474 used for the reconstruction of ancestral geographic ranges, but are also useful for reconstructing  
475 ancestral elevational ranges and migratory behavior, as the evolution of these traits parallels the  
476 modeled processes of geographic range evolution. We assessed model fit using the Akaike

477 Information Criterion (AIC). We pruned a small number of redundant tips so that a single tip  
478 represents each species. Trait scoring drew primarily upon Handbook of the Birds of the World  
479 Alive (del Hoyo et al., 2018), supplemented by regional field guides, primary literature, and in a  
480 few cases, critically evaluated eBird (Sullivan et al., 2009) records. This information was applied  
481 within the framework of IOC v 9.2 (Gill & Donsker, 2019) species limits (except for noted  
482 exceptions — see Supplementary File 6).

483 Species' geographic ranges were defined as their breeding distributions within nine  
484 biogeographic regions (Supplementary File 4): Palearctic, Indomalaya, Philippines, Wallacea,  
485 Australo-Papua, Bismarcks + Solomons, Pacific, Afrotropics, and Americas. Our definition of the  
486 ambiguous boundary between the Palearctic and Indomalayan regions follows Udvardy (1975), and  
487 we set the precise boundary along the Himalayas at the freezing line (White et al., 2019). We did  
488 not score species as inhabiting regions where they occur extremely marginally relative to their  
489 overall range. The certainty in nodal states for the reconstruction of *Turdus* (Turdidae) was  
490 confounded by the inclusion of a single species (*Turdus poliocephalus*) that occurs across six Indo-  
491 Pacific island regions in an otherwise strictly Eurasian clade. To address this, we lumped  
492 Philippines, Wallacea, Bismarcks + Solomons, and Pacific into a single region for that particular  
493 analysis.

494 Elevational ranges were defined as "Lowland," "Montane," or "Lowland + Montane"  
495 according to species' breeding distributions. Scoring followed essentially the same criteria used to  
496 define MIPs (Section 4.1), though research of elevational limits for each species was by necessity  
497 less rigorous than for MIPs in the focal archipelagos. Additionally, species with geographically  
498 disjunct lowland and montane populations — whether on different islands or the same landmass —  
499 were scored "Lowland + Montane."

500 Migratory behavior was categorized as "Sedentary," "Short-distance Migration," and  
501 "Long-distance Migration." "Short-distance Migration" includes a spectrum of movement from  
502 nomadism and altitudinal migration to annual migratory movements up to 2,000 km. "Long-  
503 distance Migration" is defined as regular migratory movements over 2,000 km. Species were scored  
504 for all categories of movement shown by their constituent populations.

505

#### 506 **4.4. Geographic origin of species**

507 We attempted to identify respective Eurasian (Palearctic + Indomalaya) or Australo-Papuan  
508 ancestral origin for the 80 species with MIPs that were included in geographic reconstructions. We

509 defined individual species' ancestral origins by counting back from terminal tree nodes until  
510 reaching "Ancestral Source Nodes" with  $> 75\%$  probability of being either Eurasian or Australo-  
511 Papuan. Species for which the 75% threshold was not crossed in the reconstructions do not have  
512 clear ancestral origins in either source region, and these were not considered further.

513 We wanted to test the hypothesis that features of the area of ancestral origin influence  
514 the pattern and process of MIP formation in archipelagos. We are therefore concerned with  
515 ancestral ranges that are largely restricted to (not merely inclusive of) Eurasia or Australo-Papua.  
516 This is reflected in our treatment of the reconstructed ancestral range probabilities for this exercise,  
517 specifically that we divided composite region scores into their individual constituent parts. For  
518 example, if a reconstructed node had a 100% probability of "Australo-Papua + Wallacea", we  
519 treated that node as being 50% Australo-Papuan and 50% Wallacean.

520 The Eurasian ancestral source pool of island colonists includes both temperate  
521 elements (e.g., Sino-Himalayan mountains) and tropical elements (e.g., South and Southeast Asia).  
522 We hypothesized that lineages with temperate origins and preadaptations to cold and seasonal  
523 environments are better able to directly colonize island mountains. To estimate the respective  
524 temperate vs. tropical evolutionary backgrounds of Eurasian-origin MIPs, we plotted the posterior  
525 probabilities of a Palearctic or Indomalayan ancestral area back through time. For this exercise we  
526 did not divide composite region scores as described above.

527

## 528 **4.5. Statistical analyses**

529

### 530 **4.5.1. Montane vs. lowland ancestry**

531 To establish whether Eurasian-origin and Australo-Papuan-origin species evolved from lowland or  
532 montane continental ancestors, and whether there was a difference between the two groups, we used  
533 the reconstructed probabilities of montane distribution for the Ancestral Source Nodes of each  
534 species. In some cases, models reconstructed simultaneous lowland and montane distributions for  
535 the Ancestral Source Node, typically with low probability. Here we split the combined  
536 "Montane/Lowland" probabilities evenly, so that 50% of the probability was attributed to the  
537 overall "Montane" score, and 50% to the overall "Lowland" score. Mann-Whitney U-tests were  
538 used to compare probabilities of lowland vs. montane ancestry between the Eurasian and Australo-  
539 Papuan groups.

540

541 **4.5.2. Establishing multiple MIPs**

542 We tallied the number of MIPs for each species, and tested whether Eurasian-origin and Australo-  
543 Papuan-origin species differ in their capacity to establish multiple MIPs. Species dispersing from  
544 the respective source regions into the archipelagos have had different possibilities for island  
545 colonization and MIP formation. Important varying factors include the number, sizes, heights, and  
546 geographic configuration of proximate islands, and past inter-island connectivity via land bridges.  
547 To help control for these differences, we additionally made separate MIP counts for Wallacea and  
548 Bismarcks/Solomons, and conducted analyses both for all islands, and for the separate island  
549 groups. We tested for differences in number of MIPs between Eurasian-origin vs. Australo-Papuan-  
550 origin species using Mann-Whitney U-tests. We additionally tested for differences in the proportion  
551 of Eurasian-origin vs. Australo-Papuan species having > 1 MIP using chi-squared tests.

552 Species with high numbers of MIPs often have continental populations in Eurasia, an  
553 observation which may be useful for understanding the processes by which Eurasian-origin MIPs  
554 form (only two Australo-Papuan-origin species have both MIPs and continental populations). To  
555 quantify this pattern, we tested whether species with both continental and island populations have  
556 more MIPs than species entirely restricted to islands. Occurrence of Eurasian-origin species in  
557 Australo-Papua was not considered to constitute “continental occurrence.” Comparison of medians  
558 was made using a Mann-Whitney U-test.

559

560 **4.5.3. MIPs and LIPs**

561 Montane diversity on tropical islands may be the result of taxon cycles (Wilson, 1959, 1961;  
562 Ricklefs & Cox, 1978; Ricklefs & Bermingham, 2002). According to this idea, lowland island  
563 radiations gradually adapt to forests of island interiors, shift elevational distributions upwards,  
564 experience extinctions in smaller islands, and relictualize as widely separated montane species.  
565 Ongoing taxon cycles would presumably leave a signature in the proportion of MIPs to lowland  
566 island populations (LIPs). For a given lineage, early stages of taxon cycles should be numerically  
567 dominated by LIPs, with relatively few MIPs. As cycles progress, numbers of LIPs and MIPs  
568 should become more similar, assuming attainment of montane ranges is not perfectly synchronized  
569 across populations. In the late stages of taxon cycles, single-island endemics should form, at which  
570 stage the MIP/LIP signature becomes non-informative, as it is identical to a species that has evolved  
571 via direct colonization by a montane ancestor.

572                    We examined elevational niche conservatism and looked for evidence of taxon cycles  
573                    by analyzing the ratios of MIPs to total island populations (MIPs + LIPs) for species of Eurasian-  
574                    origin and Australo-Papuan-origin, respectively. LIPs were defined as populations with elevational  
575                    ranges extending below 100 masl within the focal regions. These were identified for all Eurasian-  
576                    origin and Australo-Papuan-origin species with MIPs, following a process similar to that used for  
577                    MIP identification (see Section 4.1). Certain island populations were removed from the analysis if  
578                    no elevational distribution data were available, and the island in question has highlands extensive  
579                    enough to plausibly support a montane population. We did not include species with only one MIP  
580                    and no LIPs in the analysis for the reason stated above. Comparison of proportions was performed  
581                    for Eurasian-origin vs. Australo-Papuan-origin species using a Mann-Whitney U-test.  
582

#### 583                    **4.5.4. Migration**

584                    Lineages from regions with cold and seasonal climates appear better able to make broad and rapid  
585                    colonization across mountain ranges than tropical lineages (Lobo & Halffter, 2000; Donoghue,  
586                    2008; Merckx et al., 2015). Any specific traits of temperate lineages that promote colonization  
587                    across mountain ranges presumably vary between organism groups. In birds, an obvious candidate  
588                    trait linked with birds' mobility is migratory capacity. We tested whether the Eurasian ancestors of  
589                    species with MIPs are in fact more migratory than Australo-Papuan ancestors. Although migration  
590                    is widespread in Eurasia, lineages in South and Southeast Asia (which directly feed the focal  
591                    archipelagos) show very little migratory behavior. To determine whether Eurasian-origin and  
592                    Australo-Papuan-origin species evolved from migratory or sedentary continental ancestors, and  
593                    whether there was a difference between the two groups, we used the reconstructed probabilities of  
594                    migratory behavior for the Ancestral Source Nodes of each species. We calculated the total  
595                    probability that the ancestral species showed each category of migratory behavior. For example, the  
596                    probability of "Sedentary" was calculated by the summing the probabilities of the states Sedentary,  
597                    Sedentary+Short, Sedentary+Long, and Sedentary+Short+Long. Comparison of median  
598                    probabilities for Eurasian-origin versus Australo-Papuan-origin species was made using a Mann-  
599                    Whitney U-test.

600                    Species' ability to form multiple MIPs may be linked to their capacity for short-  
601                    distance migration, specifically; some of the most effective colonizers of island mountains have  
602                    short-distance migrant populations within their global ranges. To explore this idea, we tested  
603                    whether species with short-distance migrant populations form more MIPs than species that are

604 sedentary throughout their range. Note that these short-distance migrant populations exist  
605 exclusively outside of the focal archipelagos. We first analyzed all species with MIPs throughout  
606 the focal archipelagos, including species not sampled in our trees, and then separately analyzed  
607 Eurasian-origin species only (no Australo-Papuan-origin species have populations with short-  
608 distance migration). Comparisons of medians were made using Mann-Whitney U-tests.

609

#### 610 **4.5.5. Competitive pressure in the lowlands**

611 Competitive pressure from closely related species may drive the formation of montane populations  
612 (Terborgh, 1971). To assess the degree of this pressure in our study system, we determined whether  
613 individual MIPs shared islands with breeding species from the same genus and family (respectively)  
614 occurring in the lowlands (i.e., elevational range extends below 100 masl). Genus- and family-level  
615 taxonomic classification follows IOC v 9.2 (Gill & Donsker, 2019), but we treated *Lichmera*  
616 *lombokia* and *Melidectes whitemanensis* (Meliphagidae) as monotypic genera based on the results  
617 of Marki et al. (2017). We compared the respective competitive pressure faced by Eurasian-origin  
618 versus Australo-Papuan MIPs using chi-squared tests.

619

#### 620 **4.5.6. Phylogenetic null models**

621 We created a single phylogenetic tree that included all 80 species with MIPs whose DNA sequences  
622 were compared (see Section 4.2). Using a well-resolved, dated ultraconserved element (UCE)  
623 phylogenetic tree of passerine families (Oliveros et al., 2019) as a backbone, we pruned our clade-  
624 level trees and bound the relevant tips to this tree. We assessed how well the empirical patterns of  
625 the tests above could be replicated based on data simulated under a Brownian motion model of  
626 evolution in this tree. This was done to assess how well our results are explained by phylogenetic  
627 history alone, in the absence of direct quantification of geographic or ecological characters among  
628 lineages. To perform these null models, we first tested the phylogenetic signal in the variables  
629 described in Sections 4.5.1–4.5.5 using Pagel’s  $\lambda$  (Pagel, 1999), also quantifying the  $\sigma^2$  values using  
630 fitContinuous function in the R package geiger (v.2.0; Pennell et al., 2014). The maximum  
631 likelihood value of  $\lambda$  was used to transform the species-level tree using the transformPhylo function  
632 in motmot (v.2.1.3; Puttik et al., 2019). Next, using the  $\sigma^2$  values for each variable, we simulated  
633 1,000 null species-level datasets on the transformed trees, using the fastBM function in phytools  
634 (v.0.7-70; Revell, 2020). We then performed one-way ANOVA tests on the empirical data and null  
635 datasets, and compared the empirical F statistics against the distributions of the simulated F

636 statistics to assess the divergence in the trait values among groupings. P-values were calculated by  
637 determining the number of simulated F statistics higher than the empirical F statistic, and dividing  
638 this value by the total number of simulations (1,000).

639

640 **4.6. Taxon sampling of montane supercolonizers**

641 Among the birds inhabiting the focal archipelagos, certain species have an extraordinarily high  
642 capacity to disperse between and colonize the mountains of different islands. Reconstructing the  
643 evolutionary histories of these ‘montane supercolonizers’ can shed light on how lineages entered  
644 archipelagic mountains, and provide insight into the nature of mountain-to-mountain dispersal. We  
645 made detailed population studies of three species or clades representing montane supercolonizers:  
646 Indo-Pacific *Phylloscopus* leaf warblers (Phylloscopidae), Snowy-browed Flycatcher *Ficedula*  
647 *hyerythra* (Muscicapidae), and Mountain Tailorbird *Phyllergates cucullatus* (Cettiidae). These are  
648 small (6–12 g) insectivores with ranges spanning continental Eurasia and Indo-Pacific archipelagos,  
649 showing very subtle morphological differentiation between populations. Available evidence  
650 (Alström et al., 2011, 2018; Moyle et al., 2015) suggests continental Asian ancestral origins for all  
651 three. The population studies were designed to answer several key questions. Are the three  
652 species/clades monophyletic, and do they represent single or multiple species? Are island radiations  
653 the product of west-to-east ‘stepping-stone’ dispersal, or do modern island populations represent  
654 previously migratory populations that have become resident? How did radiations proceed through  
655 time? And what are the evolutionary relationships of the few lowland or migratory populations?

656 Our sampling provided broad geographic coverage for each species/clade, while  
657 complementing the taxonomic coverage of sequence data already available from GenBank. We  
658 sought sequence data from every subspecies of each species/clade, as well as major geographically  
659 disjunct populations within those subspecies. This approach allowed us to perform multi-gene  
660 phylogenetic analyses with near complete taxonomic coverage, as well as separate, more powerful  
661 genomic analyses drawing exclusively on our own data. Detailed summary statistics on taxonomic  
662 sampling are presented in the following sections and in Table S6.

663 In addition to the montane supercolonizers, we sampled eight further individual birds  
664 (Supplementary File 7) from three families to expand the trees used for ancestral state  
665 reconstructions (Section 4.2).

666

667 **4.6.1. Indo-Pacific *Phylloscopus* leaf warblers**

668 The Indo-Pacific leaf warblers represent a large species complex distributed from the Greater  
669 Sundas and the Philippines through Wallacea; across New Guinea and some outlying islands; and  
670 through the Bismarcks and Solomons. All populations are allopatric except for Kolombangara Leaf  
671 Warbler *P. amoenus* and Island Leaf Warbler *P. maforensis pallescens*, which co-occur on  
672 Kolombangara in the Solomons (Dutson, 2011). Populations are essentially sedentary and montane  
673 apart from a few populations that reach the lowlands on small islands. The complex is probably  
674 monophyletic, but a comprehensive phylogenetic analysis is lacking (though see Jones & Kennedy,  
675 2008; Alström et al., 2018; Ng et al., 2018; Rheindt et al., 2020). Species limits within the group are  
676 unclear, and treatment by different taxonomic authorities varies significantly. IOC 9.2 (Gill &  
677 Donsker, 2019) recognizes eight species in this complex: *P. trivirgatus* (4 subspecies), *P. nigrorum*  
678 (7 subspecies), *P. presbytes* (2 subspecies), *P. rotiensis* (monotypic), *P. makirensis* (monotypic), *P.*  
679 *sarasinorum* (2 subspecies), *P. amoenus* (monotypic), and *P. maforensis* (18 subspecies). Another  
680 two taxa were recently described from the Wallacean islands of Peleng and Taliabu (Rheindt et al.,  
681 2020). Of these, we sampled 6 of 8 species and 25 of 35 subspecies; additional GenBank data  
682 increased coverage to 7 of 8 species, and 100% of subspecies. Missing is the monotypic Rote Leaf  
683 Warbler *Phylloscopus rotiensis* from the Lesser Sundas.

684

#### 685 **4.6.2. Snowy-browed Flycatcher *Ficedula hyperythra***

686 Snowy-browed Flycatcher occurs from the Himalayas west of Nepal through southern China and  
687 Taiwan; and across Indochina, the Greater Sundas, and Wallacea. Populations in the Philippines  
688 have recently been shown not to belong to this species (Moyle et al., 2015). It has a uniformly  
689 montane breeding distribution, but is an altitudinal migrant in the Himalayas. Fourteen subspecies  
690 are recognized, including a newly described taxon from Taliabu (Rheindt et al., 2020). We sampled  
691 12 individuals representing 9 of 14 subspecies; supplementary GenBank data increased coverage to  
692 13 of 14 subspecies, missing only subspecies *mjobergi* from the Pueh Mountains of western  
693 Borneo. We additionally sampled Damar Flycatcher *Ficedula henrici*, endemic to a single small  
694 island in the Lesser Sundas, which bears morphological and vocal similarities to *F. hyperythra*, but  
695 has not previously been included in any molecular phylogenetic study.

696

#### 697 **4.6.3. Mountain Tailorbird *Phyllergates cucullatus***

698 Mountain Tailorbird is not a true tailorbird (genus *Orthotomus*, family Cisticolidae); rather, it is  
699 part of the family Cettiidae, in the genus *Phyllergates* (Alström et al., 2011), which it shares with

700 one other species from Mindanao. It occurs from the eastern Himalayas through southern China,  
701 and Indochina; across the Greater Sundas and Wallacea; and on Palawan and Luzon in the  
702 Philippines. Its breeding distribution is exclusively montane, but Himalayan populations are  
703 altitudinal migrants. Sixteen subspecies are recognized, including two newly described taxa from  
704 Peleng and Taliabu (Rheindt et al., 2020). We sampled 15 individuals representing 11 of 16  
705 subspecies; additional GenBank data increased subspecies coverage to 100%.

706

#### 707 **4.7. Library preparation and sequencing**

708 We used Illumina sequencing to generate genomic data for the population studies of the three  
709 montane supercolonizers. We sequenced ND2 from eight additional individuals in order to expand  
710 the taxonomic coverage of the ancestral state reconstructions. Raw reads have been deposited at the  
711 NCBI Sequence Read Archive (SRA). Individual nuclear and mitochondrial genes have been  
712 deposited on GenBank. Accession numbers are given in Supplementary File 7 [pending].

713

##### 714 **4.7.1. Illumina sequencing**

715 Genomic DNA was extracted both from footpad samples ( $n = 51$ ) and from fresh blood and tissue  
716 samples ( $n = 18$ ). Protocol for extracting DNA from footpad samples followed Irestedt et al. (2006).  
717 To create sequencing libraries suitable for Illumina sequencing of footpad DNA extracts, we  
718 followed the protocol of Meyer and Kircher (2010). In short, library preparation consisted of blunt-  
719 end repair, adapter ligation, and adapter fill-in, followed by four independent index PCRs. The  
720 libraries were run on half a lane on Illumina HiSeq X (pooled at equal ratio with other museum  
721 samples). For fresh samples, genomic DNA was extracted with KingFisher Duo magnetic particle  
722 processor (ThermoFisher Scientific) using the KingFisher Cell and Tissue DNA Kit. Library  
723 preparation (using Illumina TruSeq DNA Library Preparation Kit) and sequencing on Illumina  
724 HiSeqX (2x151 bp) was performed by SciLifeLab.

725

##### 726 **4.7.2. ND2 sequencing and assembly**

727 For seven fresh tissue samples, ND2 (1,041 bp) was sequenced in a single fragment. For a single  
728 footpad sample (from *Pachycephala johni* AMNH 658812), ND2 was sequenced in seven  
729 overlapping fragments of < 200 bp. Sequences were assembled using Sequencher v.4.7, and  
730 checked for stop codons or indels that would have disrupted the reading frame, and indicated  
731 amplification of pseudogenes.

732

733 **4.8. Bioinformatics**

734 **4.8.1. Read cleaning**

735 Illumina sequencing reads were cleaned using a custom-designed workflow (available at  
736 [https://github.com/mozesblom/NGSdata\\_tools](https://github.com/mozesblom/NGSdata_tools)) to remove adapter contamination, low-quality bases  
737 and low-complexity reads. Overlapping read pairs were merged using PEAR (v.0.9.10; Zhang et al.,  
738 2014), and Super Deduper (v.1.4; Petersen et al., 2015) was used to remove PCR duplicates.  
739 Trimming and adapter removal was done with TRIMMOMATIC (v.0.32; Bolger et al., 2014;  
740 default settings). Overall quality and length distribution of sequence reads was inspected with  
741 FASTQC (v.0.11.5; Andrews, 2010), both before and after cleaning.

742

743 **4.8.2. Mitochondrial genome reconstruction and mapping of individual nuclear loci**

744 Mitochondrial genomes were assembled using an iterative baiting and mapping approach  
745 (MITObim v.1.8; Hahn et al., 2013; default settings). MITObim locates initial regions of similarity  
746 between a target library and a distant reference (reference sequences are listed in Table S7). It then  
747 employs an iterative mapping strategy to locate reads overlapping with these initial segments,  
748 without using the initial reference. Resulting assemblies were corrected and validated by mapping  
749 all sequence reads against the inferred assembly using BWA mem (Li & Durbin, 2009; default  
750 settings), and checked for remaining variants and major coverage differences that might suggest  
751 MITObim had chain-linked a non-mitogenome region. We utilized the complete reconstructed  
752 mitochondrial genomes, but also extracted individual mitochondrial genes for certain analyses.

753 Individual nuclear loci were recovered from the cleaned reads by mapping directly  
754 against reference genes (see Table S7). Reference sequences were indexed using BWA (v.0.7.12; Li  
755 & Durbin, 2009) and SAMtools (v.0.1.19; Li et al., 2009). Consensus sequences were calculated  
756 using ANGSD (Korneliussen et al., 2014).

757

758 **4.8.3. Extraction of homologous gene regions**

759 In order to compare homologous regions in a phylogenomic analysis, we relied on reference data  
760 published by Jarvis et al. (2015). The data are from a broad selection of bird species and consists of  
761 individual multiple-sequence alignments from approximately 19,000 single-copy genes. The Jarvis  
762 et al. data were filtered on length, and we retained 17,341 alignments with a length of 200–5,000  
763 bp. Our filtered Illumina data (Section 4.8.1) was first assembled with Megahit (v.1.2.8; Li et al.,

764 2015), using default settings. Next, homologous regions corresponding to the multiple sequence  
765 alignments in the reference data were located and extracted from the genome assemblies. This was  
766 done using HMMer (v.3.2.1; Wheeler & Eddy, 2013), as implemented in the BirdScanner workflow  
767 (<https://github.com/Naturhistoriska/birdscanner>).

768

#### 769 **4.9. Phylogenetic analyses of montane supercolonizers**

##### 770 **4.9.1. 5–7-gene supermatrix analyses**

771 We built supermatrix trees (Sanderson et al., 1998; de Queiroz & Gatesy, 2007) for each of the  
772 three montane supercolonizers, complementing existing sequence data from GenBank with our own  
773 sampling (Supplementary File 7). We used as a foundation three phylogenetic datasets produced for  
774 the ancestral state reconstructions: those for *Phylloscopus* (Phylloscopidae), *Ficedula*  
775 (Muscicapidae), and Cettiidae (see Section 4.2). We retained the gene sets from those datasets (5–7  
776 nuclear and mitochondrial genes), but sampled many more individuals and taxa from the groups of  
777 interest. Note that the *Phylloscopus* tree used for ancestral state reconstructions included all  
778 available individuals and taxa, so it was reused without further additions. Phylogenetic analyses  
779 were performed as described in Section 4.2. We used linked substitution models for mitochondrial  
780 genes: GTR+I+G for *Phylloscopus*, and GTR for *Ficedula* and Cettiidae.

781

##### 782 **4.9.2. Mitochondrial genome analyses**

783 We performed phylogenetic analyses on the newly generated mitochondrial genome data from each  
784 of the three montane supercolonizers. Analyses were performed as described in Section 4.2. To  
785 obtain absolute date estimates, we partitioned the cyt-b and ND2 data, and applied substitution rates  
786 from Lerner et al. (2011). We used the GTR nucleotide substitution model. Outgroups were  
787 *Phylloscopus claudiae* for the Indo-Pacific *Phylloscopus* analysis; *Ficedula zanthopygia* for the  
788 *Ficedula hyperythra* analysis; and *Horornis parens* for the *Phylloctetes cucullatus* analysis, based  
789 on Alström et al. (2018); Moyle et al. (2015) and Hooper et al. (2016); and Alström et al. (2011),  
790 respectively.

791

##### 792 **4.9.3. Phylogenomic analyses**

793 Putative homologous gene regions were extracted from all genome assemblies, and aligned  
794 individually using MAFFT (v.7.310; Katoh & Standley, 2013) with the `--auto` option for  
795 automatic algorithm selection, followed by a filtering step using BMGE (v.1.12; Criscuolo &

796 Gribaldo, 2010), where uncertain alignment regions are removed. The *Phyllergates cucullatus*  
797 *meisei* individual was removed as it showed a high proportion of missing data. Gene trees were then  
798 inferred using RAxML-NG (v.0.9.0; Kozlov et al., 2019) using the GTR+G model. Alignments  
799 were then further filtered by identifying and removing long-branch taxa using TreeShrink (v.1.3.3;  
800 Mai & Mirarab, 2018), followed by a final round of MAFFT, BMGE, and RAxML-NG. The final  
801 set of gene trees were analyzed in ASTRAL III v5.6.3 (Zhang et al., 2018) to produce an estimate of  
802 a species tree. In addition, all individual gene alignments were concatenated (a total of 9,295,039  
803 bp) and a phylogeny was estimated with RAxML-NG using the GTRI+I+G model. The  
804 simultaneous inference of thousands of gene trees were facilitated by using the ParGenes v.1.0.1  
805 workflow (Morel et al., 2019), and using the GNU parallel library (Tange, 2018). Complete analysis  
806 workflow is available from GitHub [pending].

807

808

809 **SUPPLEMENTARY MATERIAL**

810 **Supplementary File 1.** Detailed results of population studies of montane supercolonizers; Figs.  
811 S1–S15; Tables S1–S7.

812

813 **Supplementary File 2.** Species distributions, region assignments, co-occurrence patterns, and  
814 migratory behavior.

815

816 **Supplementary File 3.** Species-level phylogenetic trees.

817

818 **Supplementary File 4.** Ancestral state reconstructions: geographic range, elevational range, and  
819 migratory behavior.

820

821 **Supplementary File 5.** Ancestral geographic range curves for Eurasian-origin species.

822

823 **Supplementary File 6.** Species-level phylogenetic analyses: gene sampling, settings, etc.

824

825 **Supplementary File 7.** Specimen and sequence data accession information.

826

827

828

829 **ACKNOWLEDGMENTS**

830 Genetic samples were kindly provided by the following institutions: the American Museum of  
831 Natural History, New York, NY (Paul Sweet, Tom Trombone and Peter Capainolo); the Australian  
832 National Wildlife Collection (Leo Joseph and Robert Palmer); the British Museum of Natural  
833 History, Tring (Robert Prys-Jones, Hein van Grouw and Mark Adams); Museum für Naturkunde,  
834 Berlin (Sylke Frahnert and Pascal Eckhoff); the Natural History Museum of Denmark (Jan Bolding  
835 Kristensen); Rijksmuseum van Natuurlijke Histoire, Leiden (Steven van der Mije and Pepijn  
836 Kamminga); the Swedish Museum of Natural History, Stockholm (Ulf Johansson); and the Yale  
837 Peabody Museum of Natural History, New Haven, CT (Kristof Zyskowski). We thank Petter Marki  
838 and Michael Le Pepke for contributing data. Leo Joseph, Frederick Sheldon, Trevor Price, and Jon  
839 Fjeldså provided valuable comments on the draft manuscript. AHR and KAJ acknowledge support  
840 from the Villum Foundation (Young Investigator Programme, project No. 15560), and KAJ was  
841 additionally funded by the Carlsberg Foundation (CF15-0078 and CF15-0079). JDK was supported  
842 by an Internationalisation Fellowship (CF17-0239) from the Carlsberg Foundation and an  
843 Individual Fellowship from Marie Skłodowska-Curie actions (MSCA-792534). PA was supported  
844 by the Swedish Research Council (2019-04486). The computations were performed on resources  
845 provided by SNIC through Uppsala Multidisciplinary Center for Advanced Computational Science  
846 (UPPMAX) under project SNIC 2017/7-212. The authors acknowledge support from the National  
847 Genomics Infrastructure in Stockholm, funded by Science for Life Laboratory, the Knut and Alice  
848 Wallenberg Foundation, and the Swedish Research Council. We also thank SNIC/Uppsala  
849 Multidisciplinary Center for Advanced Computational Science for assistance with massively  
850 parallel sequencing, and access to the UPPMAX computational infrastructure.

851

852

853 **AUTHOR CONTRIBUTIONS**

854 AHR and KAJ conceived the study. All authors contributed to build the dataset. AHR, JDK, JAAN,  
855 and KAJ developed the analytical framework. JMP, BP, MPKB, PGPE, and JAAN performed  
856 bioinformatics. AHR, JDK, JAAN, and KAJ performed the analyses. AHR led the writing, and all  
857 authors contributed to the discussion of the results and the writing of the manuscript.

858

859

860 **DATA AVAILABILITY**

861 Raw Illumina sequences are deposited in the Sequence Reads Archive, National Center for  
862 Biotechnology Information, SRA accession [pending]. Individual gene sequences are deposited on  
863 GenBank; accession numbers are provided in Supplementary File 5 [pending].

864

865

866 **REFERENCES**

867 Alström, P., Höhna, S., Gelang, M., Ericson, P. G., & Olsson, U. (2011). Non-monophyly and  
868 intricate morphological evolution within the avian family Cettiidae revealed by multilocus analysis  
869 of a taxonomically densely sampled dataset. *BMC Evolutionary Biology*, 11(1), 352.

870

871 Alström, P., Rheindt, F. E., Zhang, R., Zhao, M., Wang, J., Zhu, X., ... & Prawiradilaga, D. M.  
872 (2018). Complete species-level phylogeny of the leaf warbler (Aves: Phylloscopidae) radiation.  
873 *Molecular Phylogenetics and Evolution*, 126, 141–152.

874

875 Andrews, S. (2010). FastQC: a quality control tool for high throughput sequence data. Available  
876 from: <http://www.bioinformatics.babraham.ac.uk/projects/fastqc>

877

878 Baptista, L. F., Trail, P. W., & Horblit, H. M. (1997). Family Columbidae (Pigeons and doves). In  
879 *Handbook of the Birds of the World*, 4, 60–243. Lynx Edicions, Barcelona.

880

881 Bodawatta, K. H., Synek, P., Bos, N., Garcia-del-Rey, E., Koane, B., Marki, P. Z., ... & Jønsson, K.  
882 A. (2020). Spatiotemporal patterns of avian host-parasite interactions in the face of biogeographical  
883 range expansions. *Molecular Ecology*, 29(13), 2431–2448.

884

885 Bolger, A. M., Lohse, M., & Usadel, B. (2014). Trimmomatic: a flexible trimmer for Illumina  
886 sequence data. *Bioinformatics*, 30(15), 2114–2120.

887

888 Boyle, W. A. (2008). Can variation in risk of nest predation explain altitudinal migration in tropical  
889 birds?. *Oecologia*, 155(2), 397–403.

890

- 891 Böhning-Gaese, K., González-Guzmán, L. I., & Brown, J. H. (1998). Constraints on dispersal and  
892 the evolution of the avifauna of the Northern Hemisphere. *Evolutionary Ecology*, 12(7), 767–783.  
893
- 894 Christidis, L. Marki, P. Z., & Fjeldså, J. (2020). Infraorder Passerides and the ‘higher’ songbirds. In  
895 *The Largest Avian Radiation: The Evolution of Perching Birds, or the Order Passeriformes* 169–  
896 183. Lynx Edicions, Barcelona.  
897
- 898 Coates, B. J., & Bishop, K. D. (1997). A Guide to the Birds of Wallacea. Dove Publications,  
899 Alderley, Australia.  
900
- 901 Collar, N. J. (1997). Family Psittacidae (Parrots). In *Handbook of the Birds of the World*, 4, 280–  
902 477. Lynx Edicions, Barcelona.  
903
- 904 Criscuolo, A., & Gribaldo, S. (2010). BMGE (Block Mapping and Gathering with Entropy): a new  
905 software for selection of phylogenetic informative regions from multiple sequence alignments.  
906 *BMC Evolutionary Biology*, 10(1), 1–21.  
907
- 908 Diamond, J. M. (1972). *Avifauna of the Eastern Highlands of New Guinea*. Nuttall Ornithological  
909 Club, Cambridge, MA  
910
- 911 Diamond, J. M. (1975). Assembly of species communities. In *Ecology and evolution of species  
912 communities*. Harvard University Press, Cambridge, MA.  
913
- 914 Drummond, A. J., Suchard, M. A., Xie, D., & Rambaut, A. (2012). Bayesian phylogenetics with  
915 BEAUti and the BEAST 1.7. *Molecular Biology and Evolution*, 29(8), 1969–1973.  
916
- 917 Dutson, G. (2011). *Birds of Melanesia: Bismarcks, Solomons, Vanuatu and New Caledonia*.  
918 Christopher Helm, London.  
919
- 920 Fjeldså, J., Bowie, R. C., & Rahbek, C. (2012). The role of mountain ranges in the diversification of  
921 birds. *Annual Review of Ecology, Evolution, and Systematics*, 43, 249–265.  
922

- 923 Freeman, B. G., Scholer, M. N., Ruiz-Gutierrez, V., & Fitzpatrick, J. W. (2018). Climate change  
924 causes upslope shifts and mountaintop extirpations in a tropical bird community. *Proceedings of the*  
925 *National Academy of Sciences*, 115(47), 11982–11987.
- 926
- 927 Garg, K. M., Chattopadhyay, B., Koane, B., Sam, K., & Rheindt, F. E. (2020). Last Glacial  
928 Maximum led to community-wide population expansion in a montane songbird radiation in  
929 highland Papua New Guinea. *BMC Evolutionary Biology*, 20(1), 1–10.
- 930
- 931 Gill, F. & Donsker, D. (Eds). (2019). IOC World Bird List (v 9.2). doi: 10.14344/IOC.ML.9.2.
- 932
- 933 Gouy, M., Guindon, S., & Gascuel, O. (2010). SeaView version 4: a multiplatform graphical user  
934 interface for sequence alignment and phylogenetic tree building. *Molecular Biology and Evolution*,  
935 27(2), 221–224.
- 936
- 937 Hahn, C., Bachmann, L., & Chevreux, B. (2013). Reconstructing mitochondrial genomes directly  
938 from genomic next-generation sequencing reads—a baiting and iterative mapping approach.  
939 *Nucleic Acids Research*, 41(13), e129–e129.
- 940
- 941 Harris, R. J., & Reed, J. M. (2002). Behavioral barriers to non-migratory movements of birds.  
942 *Annales Zoologici Fennici*, 39, 275–290.
- 943
- 944 Hooper, D. M., Olsson, U., & Alström, P. (2016). The Rusty-tailed Flycatcher (*Muscicapa*  
945 *ruficauda*; Aves: Muscicapidae) is a member of the genus Ficedula. *Molecular Phylogenetics and*  
946 *Evolution*, 102, 56–61.
- 947
- 948 del Hoyo, J., Elliott, A., Sargatal, J., Christie, D. A., & de Juana, E. E. (2018). *Handbook of the*  
949 *Birds of the World Alive*. Lynx Edicions, Barcelona.
- 950
- 951 von Humboldt, A. & Bonpland, A. (1805). *Essay on the geography of plants*. (2009 Ed). University  
952 of Chicago Press, Chicago.
- 953

- 954 Irestedt, M., Ohlson, J. I., Zuccon, D., Kallersjö, M., & Ericson, P.G.P. (2006). Nuclear DNA from  
955 old collections of avian study skins reveals the evolutionary history of the Old World suboscines  
956 (Aves, Passeriformes). *Zoologica Scripta*, 35, 567–580.
- 957
- 958 Jankowski, J. E., Londoño, G. A., Robinson, S. K., & Chappell, M. A. (2013). Exploring the role of  
959 physiology and biotic interactions in determining elevational ranges of tropical animals. *Ecography*,  
960 36(1), 1–12.
- 961
- 962 Janzen, D. H. (1967). Why mountain passes are higher in the tropics. *The American Naturalist*,  
963 101(919), 233–249.
- 964
- 965 Jarvis, E. D., Mirarab, S., Aberer, A. J., Li, B., Houde, P., Li, C., ... & Avian Phylogenomics  
966 Consortium. (2015). Phylogenomic analyses data of the avian phylogenomics project. *GigaScience*,  
967 4(1), s13742–014.
- 968
- 969 Jepson, P., Jarvie, J. K., MacKinnon, K., & Monk, K. A. (2001). The end for Indonesia's lowland  
970 forests?. *Science*, 292(5518), 859–861.
- 971
- 972 Jones, A. W., & Kennedy, R. S. (2008). Evolution in a tropical archipelago: comparative  
973 phylogeography of Philippine fauna and flora reveals complex patterns of colonization and  
974 diversification. *Biological Journal of the Linnean Society*, 95(3), 620–639.
- 975
- 976 Jönsson, K. A., Borregaard, M. K., Carstensen, D. W., Hansen, L. A., Kennedy, J. D., Machac, A.,  
977 ... & Rahbek, C. (2017). Biogeography and biotic assembly of Indo-Pacific corvoid passerine birds.  
978 *Annual Review of Ecology, Evolution, and Systematics*, 48, 231–253.
- 979
- 980 Jönsson, K. A., Irestedt, M., Christidis, L., Clegg, S. M., Holt, B. G., & Fjeldså, J. (2014). Evidence  
981 of taxon cycles in an Indo-Pacific passerine bird radiation (Aves: *Pachycephala*). *Proceedings of  
982 the Royal Society B: Biological Sciences*, 281(1777), 20131727.
- 983

- 984 Katoh, K., Misawa, K., Kuma, K. I., & Miyata, T. (2002). MAFFT: a novel method for rapid  
985 multiple sequence alignment based on fast Fourier transform. *Nucleic Acids Research*, 30(14),  
986 3059–3066.
- 987
- 988 Katoh, K., & Standley, D. M. (2013). MAFFT multiple sequence alignment software version 7:  
989 improvements in performance and usability. *Molecular Biology and Evolution*, 30(4), 772–780.
- 990
- 991 Kennedy, J. D., Marki, P. Z., Reeve, A. H., Blom, M. P., Prawiradilaga, D. M., Haryoko, T., ... &  
992 Jönsson, K. A. (2022). Diversification and community assembly of the world's largest tropical  
993 island. *Global Ecology and Biogeography*, 31(6), 1078–1089.
- 994
- 995 Kershaw, A. P., Kaars, S., & Flenley, J. R. (2011). The Quaternary history of far eastern rainforests.  
996 In *Tropical rainforest responses to climatic change* (pp. 85–123). Springer, Berlin, Heidelberg.
- 997
- 998 Korneliussen, T. S., Albrechtsen, A., & Nielsen, R. (2014). ANGSD: analysis of next generation  
999 sequencing data. *BMC Bioinformatics*, 15(1), 356.
- 1000
- 1001 Kozlov, A. M., Darriba, D., Flouri, T., Morel, B., & Stamatakis, A. (2019). RAxML-NG: a fast,  
1002 scalable and user-friendly tool for maximum likelihood phylogenetic inference. *Bioinformatics*,  
1003 35(21), 4453–4455.
- 1004
- 1005 La Sorte, F. A., & Jetz, W. (2010). Projected range contractions of montane biodiversity under  
1006 global warming. *Proceedings of the Royal Society B: Biological Sciences*, 277(1699), 3401–3410.
- 1007
- 1008 Lerner, H. R., Meyer, M., James, H. F., Hofreiter, M., & Fleischer, R. C. (2011). Multilocus  
1009 resolution of phylogeny and timescale in the extant adaptive radiation of Hawaiian honeycreepers.  
1010 *Current Biology*, 21(21), 1838–1844.
- 1011
- 1012 Li, D., Liu, C. M., Luo, R., Sadakane, K., & Lam, T. W. (2015). MEGAHIT: an ultra-fast single-  
1013 node solution for large and complex metagenomics assembly via succinct de Bruijn graph.  
1014 *Bioinformatics*, 31(10), 1674–1676.
- 1015

- 1016 Li, H., & Durbin, R. (2009). Fast and accurate short read alignment with Burrows-Wheeler  
1017 transform. *Bioinformatics*, 25(14), 1754–1760.
- 1018
- 1019 Li, H., Handsaker, B., Wysoker, A., Fennell, T., Ruan, J., Homer, N., ... & Durbin, R. (2009). The  
1020 sequence alignment/map format and SAMtools. *Bioinformatics*, 25(16), 2078–2079.
- 1021
- 1022 Mai, U., & Mirarab, S. (2018). TreeShrink: fast and accurate detection of outlier long branches in  
1023 collections of phylogenetic trees. *BMC Genomics*, 19(5), 23–40.
- 1024
- 1025 Marki, P. Z., Jönsson, K. A., Irestedt, M., Nguyen, J. M., Rahbek, C., & Fjeldså, J. (2017).  
1026 Supermatrix phylogeny and biogeography of the Australasian Meliphagidae radiation (Aves:  
1027 Passeriformes). *Molecular Phylogenetics and Evolution*, 107, 516–529.
- 1028
- 1029 Matzke, N. (2013a). Probabilistic historical biogeography: new models for founder-event  
1030 speciation, imperfect detection, and fossils allow improved accuracy and model-testing. University  
1031 of California, Berkeley.
- 1032
- 1033 Matzke, N.J. (2013b). BioGeoBEARS: Biogeography with Bayesian (and Likelihood)  
1034 Evolutionary Analysis in R Scripts. University of California, Berkeley.
- 1035
- 1036 Mayr, E. (1944). The birds of Timor and Sumba. *Bulletin of the American Museum of Natural  
1037 History*, 83, 123–194.
- 1038
- 1039 Mayr, E., & Diamond, J. M. (1976). Birds on islands in the sky: origin of the montane avifauna of  
1040 northern Melanesia. *Proceedings of the National Academy of Sciences*, 73(5), 1765–1769.
- 1041
- 1042 Mayr, E., & Diamond, J. M. (2001). *The Birds of Northern Melanesia: Speciation, Ecology &  
1043 Biogeography*. Oxford University Press, New York.
- 1044
- 1045 Merckx, V. S., Hendriks, K. P., Beentjes, K. K., Mennes, C. B., Becking, L. E., Peijnenburg, K. T.,  
1046 ... & Schilthuizen, M. (2015). Evolution of endemism on a young tropical mountain. *Nature*,  
1047 524(7565), 347–350.

- 1048
- 1049 Meyer, M., & Kircher, M. (2010). Illumina Sequencing Library Preparation for Highly Multiplexed  
1050 Target Capture and Sequencing. *Cold Spring Harbor Protocols*. doi:10.1101/pdb.prot5448.
- 1051
- 1052 Morel, B., Kozlov, A. M., & Stamatakis, A. (2019). ParGenes: a tool for massively parallel model  
1053 selection and phylogenetic tree inference on thousands of genes. *Bioinformatics*, 35(10), 1771–  
1054 1773.
- 1055
- 1056 Moyle, R. G., Hosner, P. A., Jones, A. W., & Outlaw, D. C. (2015). Phylogeny and biogeography of  
1057 *Ficedula* flycatchers (Aves: Muscicapidae): novel results from fresh source material. *Molecular  
1058 Phylogenetics and Evolution*, 82, 87–94.
- 1059
- 1060 Myers, N., Mittermeier, R. A., Mittermeier, C. G., Da Fonseca, G. A., & Kent, J. (2000).  
1061 Biodiversity hotspots for conservation priorities. *Nature*, 403(6772), 853–858.
- 1062
- 1063 Ng, N. S., Prawiradilaga, D. M., Ng, E. Y., Ashari, H., Trainor, C., Verbelen, P., & Rheindt, F. E.  
1064 (2018). A striking new species of leaf warbler from the Lesser Sundas as uncovered through  
1065 morphology and genomics. *Scientific Reports*, 8(1), 1–13.
- 1066
- 1067 Oliveros, C. H., Field, D. J., Ksepka, D. T., Barker, F. K., Aleixo, A., Andersen, M. J., ... & Bravo,  
1068 G. A. (2019). Earth history and the passerine superradiation. *Proceedings of the National Academy  
1069 of Sciences*, 116(16), 7916–7925.
- 1070
- 1071 Pagel, M. (1999). Inferring the historical patterns of biological evolution. *Nature*, 401(6756), 877–  
1072 884.
- 1073
- 1074 Pennell, M. W., Eastman, J. M., Slater, G. J., Brown, J. W., Uyeda, J. C., FitzJohn, R. G., ... &  
1075 Harmon, L. J. (2014). geiger v2. 0: an expanded suite of methods for fitting macroevolutionary  
1076 models to phylogenetic trees. *Bioinformatics*, 30(15), 2216–2218.
- 1077

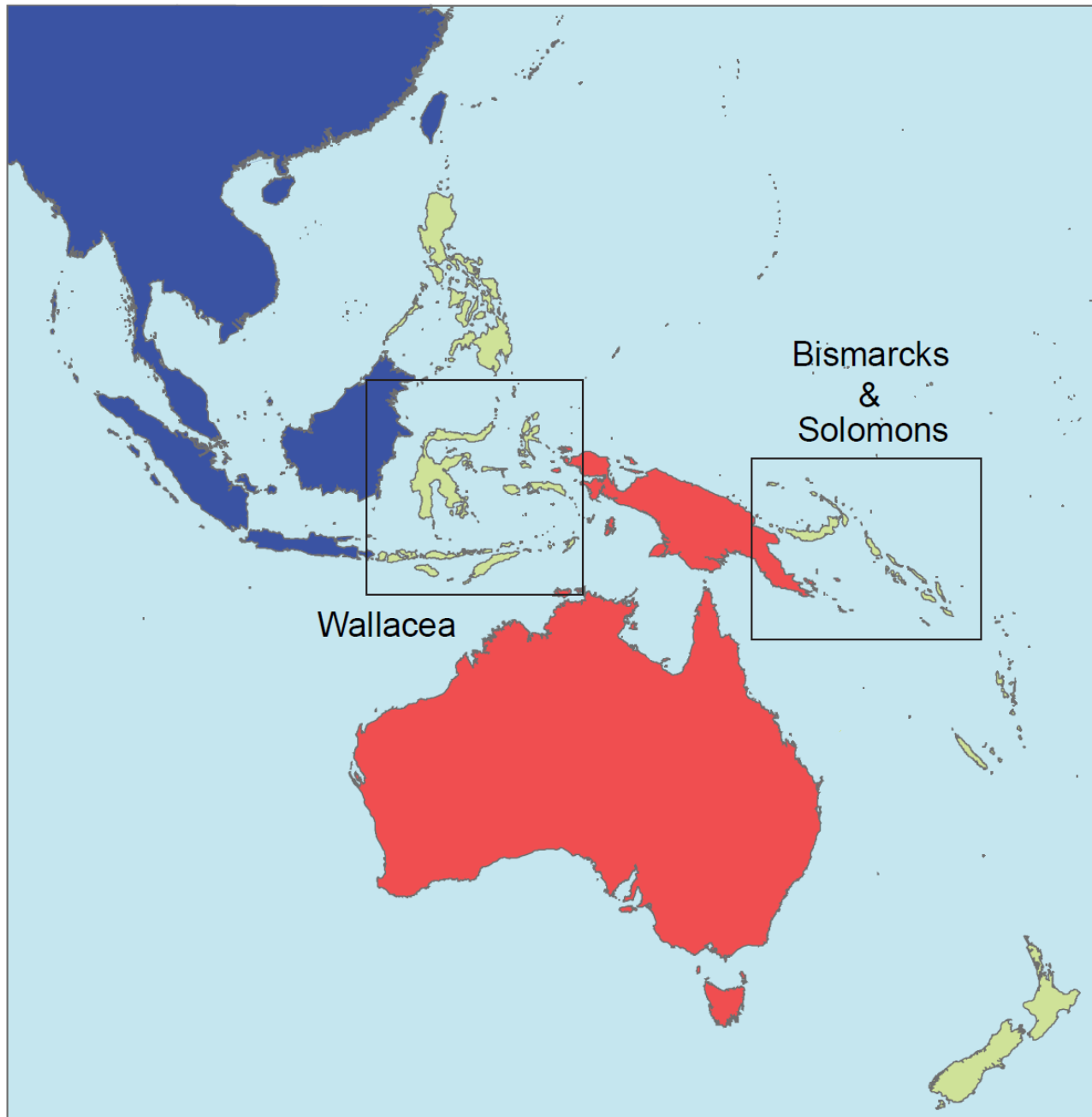
- 1078 Petersen, K. R., Streett, D. A., Gerritsen, A. T., Hunter, S. S., & Settles, M. L. (2015, September).  
1079 Super deduper, fast PCR duplicate detection in fastq files. In *Proceedings of the 6th ACM*  
1080 *Conference on Bioinformatics, Computational Biology and Health Informatics* (pp. 491–492).  
1081  
1082 Price, T. D., Hooper, D. M., Buchanan, C. D., Johansson, U. S., Tietze, D. T., Alström, P., ... &  
1083 Mohan, D. (2014). Niche filling slows the diversification of Himalayan songbirds. *Nature*,  
1084 509(7499), 222–225.  
1085  
1086 Pujolar, J. M., Blom, M. P., Reeve, A. H., Kennedy, J. D., Marki, P. Z., Korneliussen, T. S.,  
1087 Freeman, B. G., Sam, K., Linck, E., Haryoko, T., Iova, B., Koane, B., Maiah, G., Paul, L., Irestedt,  
1088 M., & Jönsson, K. A. (2022). The formation of avian montane diversity across barriers and along  
1089 elevational gradients. *Nature Communications*, 13(1), 1–13.  
1090  
1091 Puttik, M., Thomas, G., Freckleton, R., Clarke, M., Ingram, T., Orme, D., & Paradis, E. (2019).  
1092 motmot: Models of Trait Macroevolution on Trees. R package version 2.1.3. Available from:  
1093 <https://CRAN.R-project.org/package=motmot>  
1094  
1095 de Queiroz, A., & Gatesy, J. (2007). The supermatrix approach to systematics. *Trends in Ecology &*  
1096 *Evolution*, 22(1), 34–41.  
1097  
1098 Rambaut, A. & Drummond, A. J. (2015). TreeAnnotator v1.8.2: MCMC Output analysis. Retrieved  
1099 from: <http://beast.bio.ed.ac.uk>  
1100  
1101 Rambaut, A., Suchard, M. A., Xie, D. & Drummond, A. J. (2014). Tracer v1.6. Retrieved from:  
1102 <http://beast.bio.ed.ac.uk>  
1103  
1104 Ree, R. H., & Smith, S. A. (2008). Maximum likelihood inference of geographic range evolution by  
1105 dispersal, local extinction, and cladogenesis. *Systematic Biology*, 57(1), 4–14.  
1106  
1107 Revell, L. J. (2020). phytools: Phylogenetic Tools for Comparative Biology (and Other Things). R  
1108 package version 0.7-70. Available from: <https://CRAN.R-project.org/package=phytools>  
1109

- 1110 Rheindt, F. E., Prawiradilaga, D. M., Ashari, H., Gwee, C. Y., Lee, G. W., Wu, M. Y., & Ng, N. S.  
1111 (2020). A lost world in Wallacea: Description of a montane archipelagic avifauna. *Science*,  
1112 367(6474), 167–170.
- 1113
- 1114 Ricklefs, R. E., & Cox, G. W. (1978). Stage of taxon cycle, habitat distribution, and population  
1115 density in the avifauna of the West Indies. *The American Naturalist*, 112(987), 875–895.
- 1116
- 1117 Ricklefs, R. E., & Bermingham, E. (2002). The concept of the taxon cycle in biogeography. *Global  
1118 Ecology and Biogeography*, 11(5), 353–361.
- 1119
- 1120 Sanderson, M. J., Purvis, A., & Henze, C. (1998). Phylogenetic supertrees: assembling the trees of  
1121 life. *Trends in Ecology & Evolution*, 13(3), 105–109.
- 1122
- 1123 Sheldon, F. H., Lim, H. C., & Moyle, R. G. (2015). Return to the Malay Archipelago: the  
1124 biogeography of Sundaic rainforest birds. *Journal of Ornithology*, 156(1), 91–113.
- 1125
- 1126 Skutch, A. F. (1985). Clutch size, nesting success, and predation on nests of Neotropical birds,  
1127 reviewed. *Ornithological Monographs*, 36, 575–594.
- 1128
- 1129 Stresemann, E. (1939). Die Vögel von Celebes. *Journal für Ornithologie*, 87(3), 299–425.
- 1130
- 1131 Sullivan, B. L., Wood, C. L., Iliff, M. J., Bonney, R. E., Fink, D., & Kelling, S. (2009). eBird: a  
1132 citizen-based bird observation network in the biological sciences. *Biological Conservation*, 142,  
1133 2282–2292.
- 1134
- 1135 Tange, O. (2018). GNU Parallel 2018. doi:10.5281/zenodo.1146014
- 1136
- 1137 Terborgh, J. (1971). Distribution on environmental gradients: theory and a preliminary  
1138 interpretation of distributional patterns in the avifauna of the Cordillera Vilcabamba, Peru. *Ecology*,  
1139 52(1), 23–40.
- 1140

- 1141 Udvardy, M. D. F. (1975). A classification of the biogeographical provinces of the world (Vol. 8).  
1142 International Union for Conservation of Nature and Natural Resources, Morges.  
1143  
1144 Wallace, A. R. (1869). *The Malay Archipelago: the Land of the Orang-utan and the Bird of Paradise; a Narrative of Travel, with Studies of Man and Nature*. Macmillan, London.  
1145  
1146 Wheeler, T. J., & Eddy, S. R. (2013). nhmmmer: DNA homology search with profile HMMs.  
1147 *Bioinformatics*, 29(19), 2487–2489.  
1148  
1149  
1150 White, A. E., Dey, K. K., Mohan, D., Stephens, M., & Price, T. D. (2019). Regional influences on  
1151 community structure across the tropical-temperate divide. *Nature Communications*, 10(1), 1–8.  
1152  
1153 White, C. M. N., & Bruce, M. D. (1986). *The birds of Wallacea (Sulawesi, The Moluccas and Lesser Sunda Islands)*. British Ornithologists' Union, London.  
1154  
1155 Wilson, E. O. (1959). Adaptive shift and dispersal in a tropical ant fauna. *Evolution*, 13(1), 122–  
1156 144.  
1157  
1158 Wilson, E. O. (1961). The nature of the taxon cycle in the Melanesian ant fauna. *The American Naturalist*, 95(882), 169–193.  
1159  
1160  
1161 Wood, D. E., Lu, J., & Langmead, B. (2019). Improved metagenomic analysis with Kraken 2.  
1162 *Genome Biology*, 20(1), 1–13.  
1163  
1164 Zhang, C., Rabiee, M., Sayyari, E., & Mirarab, S. (2018). ASTRAL-III: polynomial time species  
1165 tree reconstruction from partially resolved gene trees. *BMC Bioinformatics*, 19(6), 15–30.  
1166  
1167 Zhang, J., Kobert, K., Flouri, T., & Stamatakis, A. (2014). PEAR: a fast and accurate Illumina  
1168 Paired-End reAd mergeR. *Bioinformatics*, 30(5), 614–620.  
1169  
1170  
1171  
1172

1173 **FIGURES & TABLES**

1174

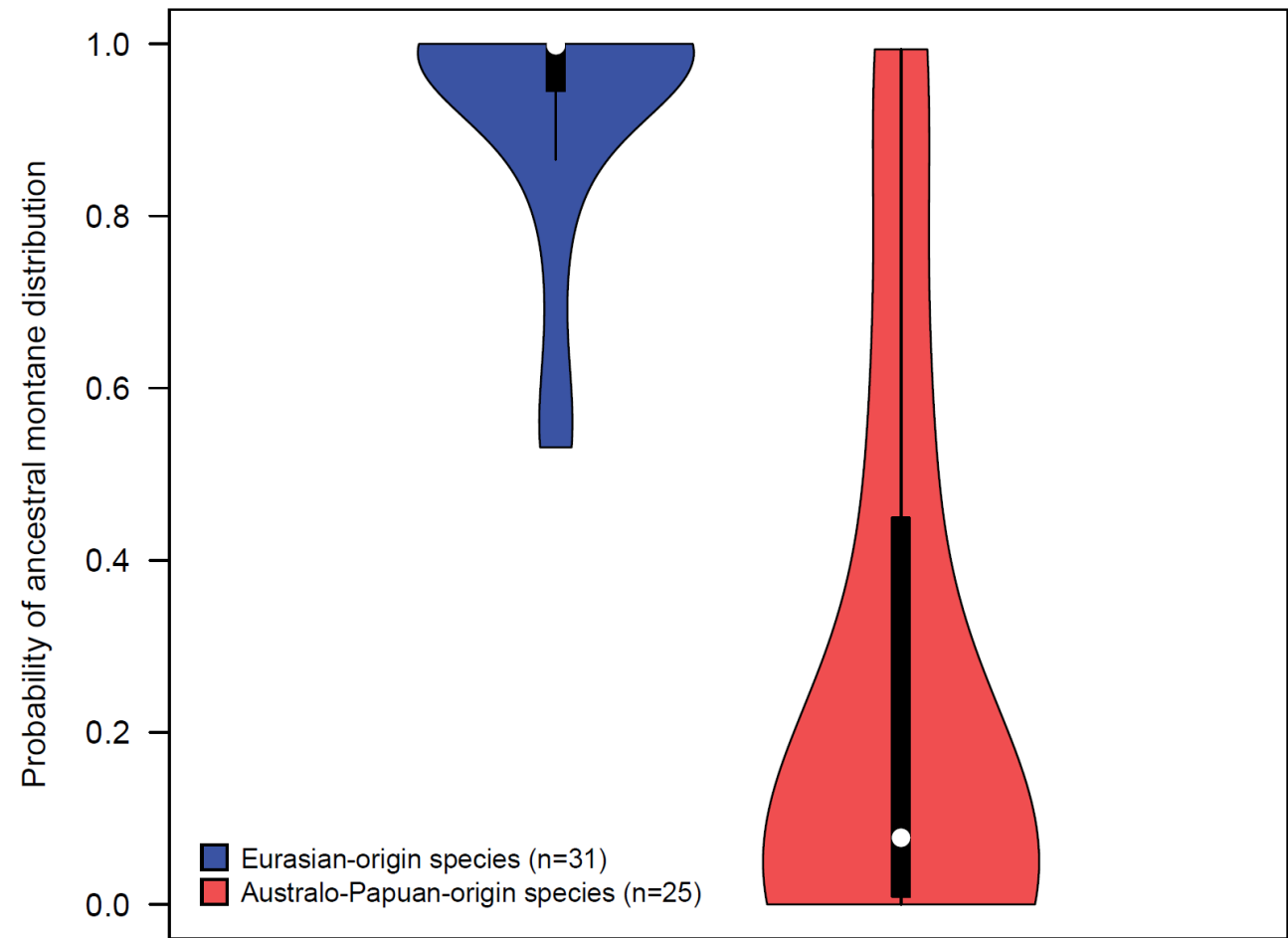


1175

1176 **Fig. 1.** Map of the study region with focal archipelagos highlighted. The colonization source pools  
1177 of Eurasia and Australo-Papua are colored blue and red, respectively.

1178

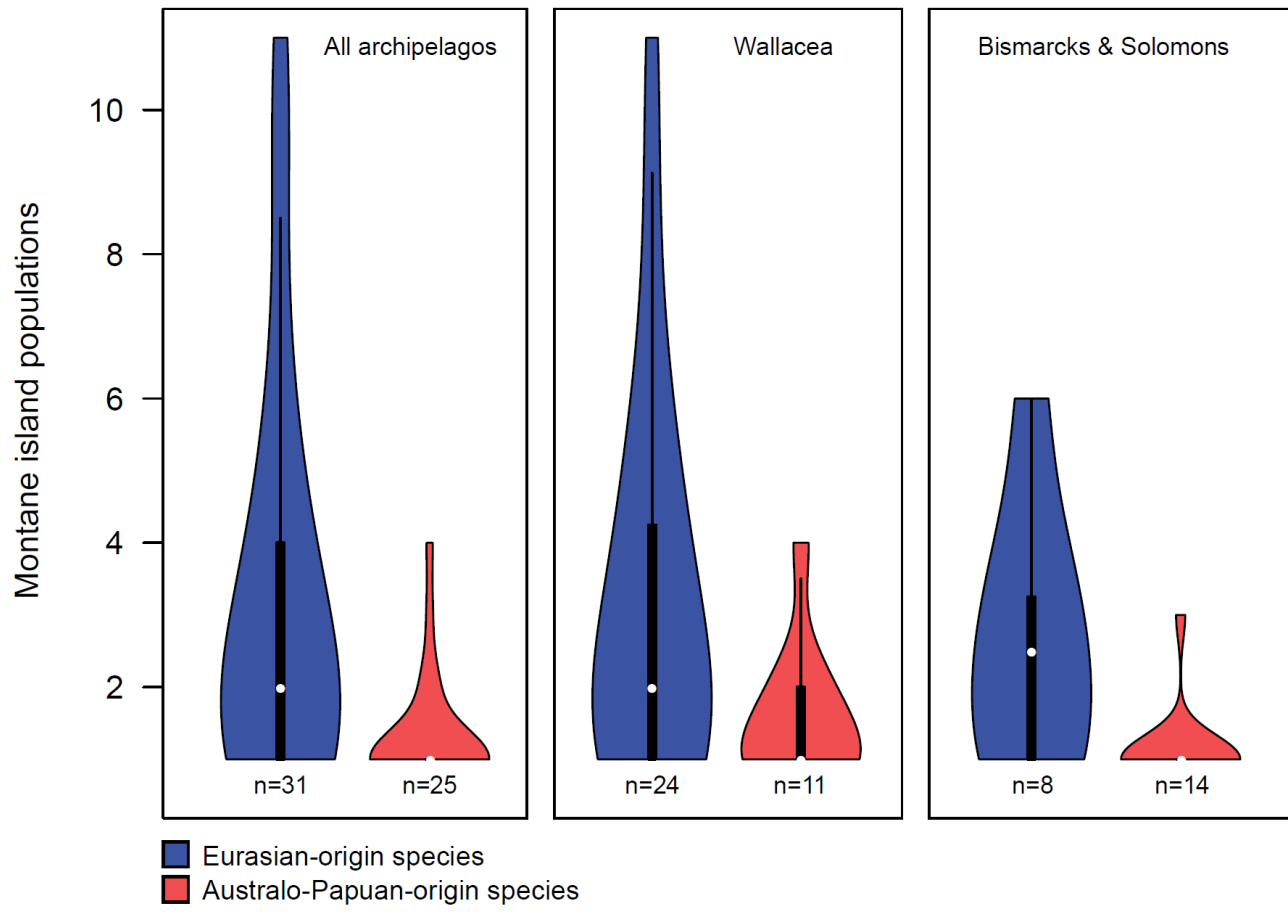
1179



1180

1181

1182 **Fig. 2.** Probability of ancestral montane distribution for Eurasian-origin versus Australo-Papuan-  
1183 origin species with montane island populations (MIPs). Values are derived from the probabilities at  
1184 the Ancestral Source Nodes of all species from the respective groups, as described in Section 4.5.1.  
1185



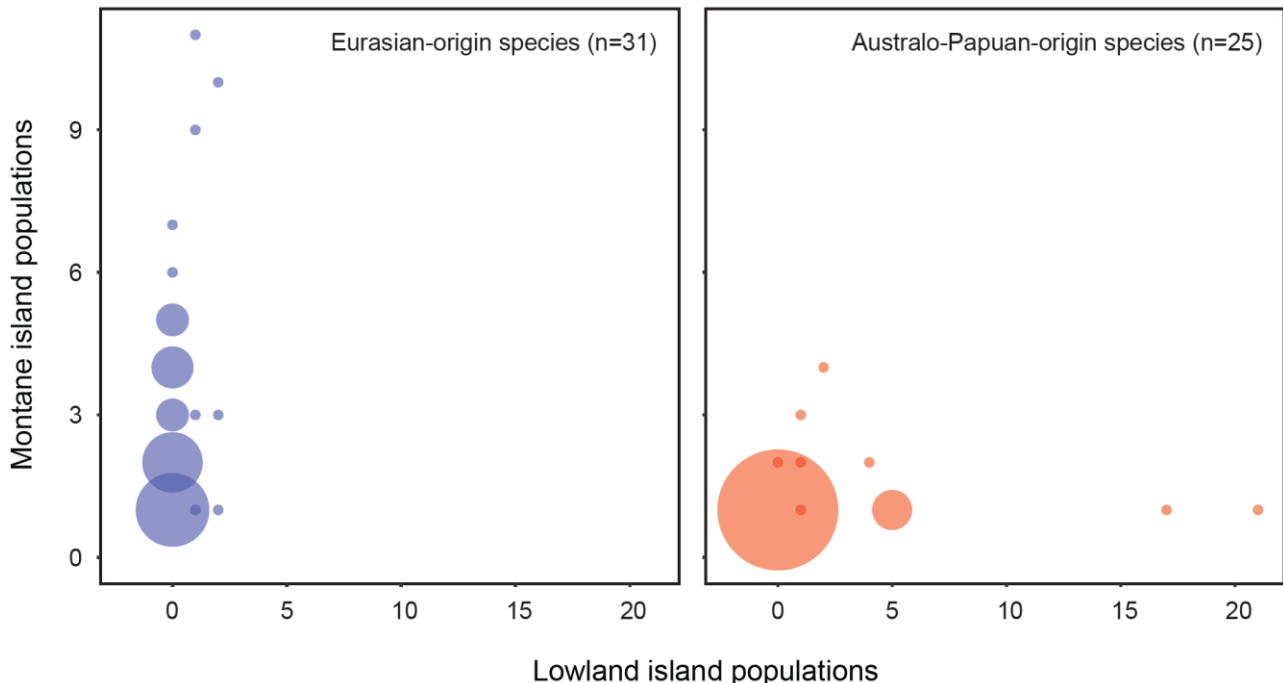
1186

1187

1188 **Fig. 3.** Number of montane island populations (MIPs) per species, by region, for Eurasian-origin  
1189 versus Australo-Papuan origin species.

1190

1191



1192

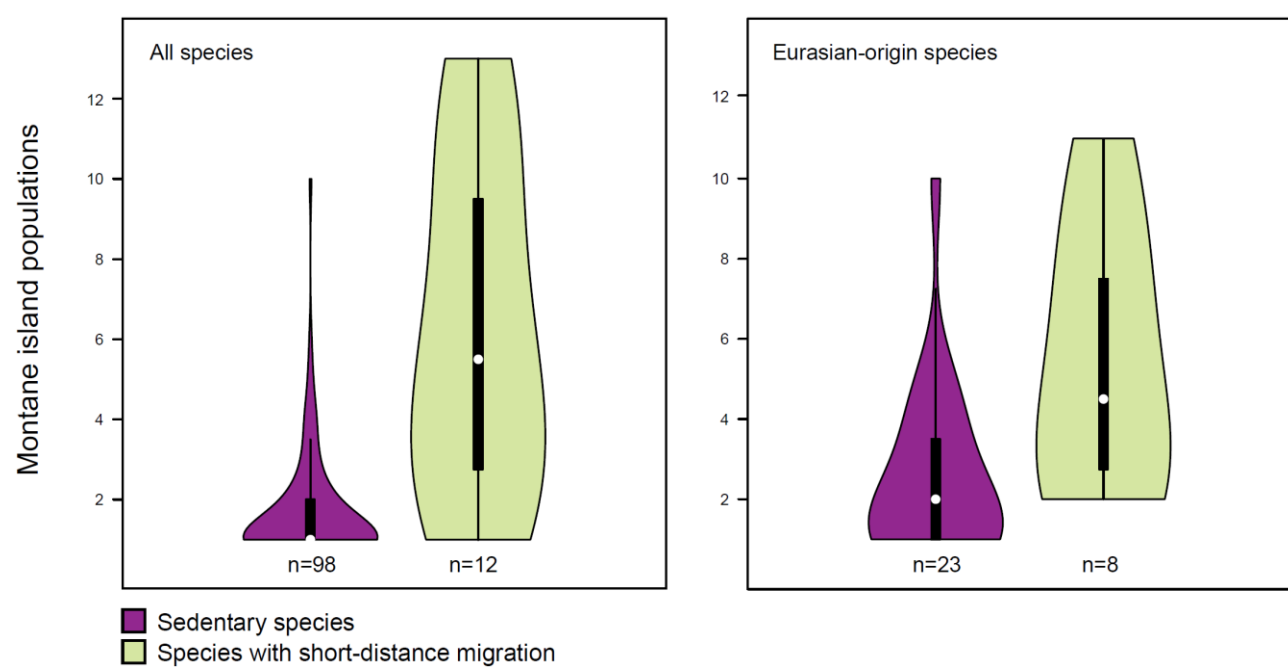
1193

1194 **Fig. 4.** Bubble plots showing number of montane island populations (MIPs) vs. lowland island  
1195 populations (LIPs) for each individual focal species. Bubble diameter reflects the number of species  
1196 sharing specific counts of MIPs vs. LIPs, from one species (smallest bubbles) to 15 species (largest  
1197 bubble); scale is consistent between the two plots. At left: Eurasian-origin species are consistently  
1198 montane across their archipelagic ranges. At right: Australo-Papuan-origin species show mixed  
1199 montane and lowland distributions; the overall pattern could reflect taxon cycles at different stages  
1200 (see Section 2.1.3).

1201

1202

1203



1204

1205

1206 **Fig. 5.** Number of montane island populations (MIPs) per species, for species with or without short-  
1207 distance migrant populations. Short-distance migrant populations occur only outside the focal  
1208 archipelagos, and no species with MIPs have long-distance migrant populations. At left: all 110  
1209 species with MIPs in the focal region, including species we did not genetically sample. At right:  
1210 Eurasian-origin species only.

1211

1212



1213

1214 **Fig. 6.** Three montane supercolonizers. From left to right: Mountain Tailorbird *Phylloscopus*  
1215 *cucullatus*, Snowy-browed Flycatcher *Ficedula hyperythra*, and a representative of an Indo-Pacific  
1216 leaf warbler clade (*Phylloscopus maforensis ceramensis*) (illustrations: Lynx Edicions).

1217

1218 **Table 1.** Species with montane island population (MIPs) in the focal archipelagos, and summary  
1219 statistics of those MIPs. Note that some species have MIPs both in Wallacea and in the  
1220 Bismarcks/Solomons.

1221

	All archipelagos	Wallacea	Bismarcks/Solomons
No. species identified	110	79	34
No. species placed in our phylogenies	80	56	26
Eurasian species	31	24	8
Australo-Papuan species	25	11	14
Other species	24	21	4
 No. MIPs identified	237	176	61
No. MIPs represented in our phylogenies	174	131	43
Eurasian MIPs	100	79	21
Australo-Papuan MIPs	33	17	16
Other MIPs	41	35	6

1222

1223

1224 **Table 2.** Ancestral migratory behavior of Eurasian-origin vs. Australo-Papuan-origin species with  
1225 MIPs. Numbers are the mean probabilities of migratory behavior classes at Ancestral Source Nodes  
1226 for all species. Migratory behavior classes are not mutually exclusive for species or ancestral nodes,  
1227 as different populations within a single species can show different migratory behavior.

1228

	Sedentary	Short-distance migrant	Long-distance migrant	Any movement
Eurasian species	0.6728	0.5512	0.0254	0.5647
Australo-Papuan species	0.9999	0.0122	0	0.0122

1229